

Thermographic Testing applied to Fiber Reinforced Polymers

by
Michael Jolibois

A THESIS

submitted to

Oregon State University

Honors College

in partial fulfillment of
the requirements for the
degree of

Honors Baccalaureate of Science in Mechanical Engineering
(Honors Scholar)

Presented March 8, 2021
Commencement June 2021

AN ABSTRACT OF THE THESIS OF

Michael Jolibois for the degree of Honors Baccalaureate of Science in Mechanical Engineering presented on March 8, 2021. Title: Thermographic Testing applied to Fiber Reinforced Polymers.

Abstract approved: _____

Mentor: Dr. Roberto Albertani

Non-destructive testing is a methodology to inspect production and operational parts for potential flaws, defects, or damages. The present work is based on pulsed wave thermography, a thermal imaging method based on heat conduction to identify surface and subsurface defects potentially present in a component. Pulsed wave thermography applies a fast pulse of heat energy on the specimen's surface while heat conduction through the material is recorded through an infrared camera. Test procedures are established with the objective of comparing system performance between homogeneous and fiber reinforced polymers. Preliminary tests on aluminum alloy have shown reliable defect detection using profile graphs with noisy data due to high metal heat conductivity. Tests on fiber reinforced polymer samples confirmed pulsed wave thermography can detect defects within carbon composites, however only surface level data can be detected in fiberglass and sandwich panels applying the basic level analysis as performed in the current work. Advanced data processing for better performance on a wider range of composites will be applied in the continuation of the research. An educational laboratory procedure for teaching the basic operation of the system in an undergraduate and graduate class environment has been developed.

Key Words: Non-destructive testing, thermography, composite, non-homogenous, homogenous, fiber reinforced polymers.

Corresponding e-mail address: joliboim@oregonstate.edu

©Copyright by Michael Jolibois
March 8, 2021

Thermographic Testing applied to Fiber Reinforced Polymers

by
Michael Jolibois

A THESIS

submitted to
Oregon State University
Honors College

in partial fulfillment of
the requirements for the
degree of

Honors Baccalaureate of Science in Mechanical Engineering
(Honors Scholar)

Presented March 8, 2021
Commencement June 2021

Honors Baccalaureate of Science in Mechanical Engineering project of Michael Jolibois presented on March 8, 2021.

APPROVED:

Roberto Albertani, Mentor, representing Oregon State University MIME

Deborah Pence, Committee Member, representing Oregon State University MIME

Josh Wilcox, Committee Member, representing External Engineering Industry

Toni Doolen, Dean, Oregon State University Honors College

I understand that my project will become part of the permanent collection of Oregon State University, Honors College. My signature below authorizes release of my project to any reader upon request.

Michael Jolibois, Author

- 1 Introductions
- 2 Background and Literature Review
 - 2.1 Historical Review
 - 2.2 Fiber Reinforced Polymers Materials
 - 2.3 Concepts of damage in Fiber Reinforced Polymers
 - 2.4 Testing of composite materials
 - 2.5 Non-destructive testing
- 3 Pulse Wave Thermography
 - 3.1 Principles and theory of pulse wave thermography
 - 3.2 Tests data post processing
 - 3.3 General testing procedure
 - 3.4 Results
- 4 Testing methods using pulse wave thermography.
 - 4.1 Homogeneous materials
 - Testing procedure
 - Specimen Design and Fabrication
 - 4.2 Non-homogeneous materials
 - Testing procedure
 - Specimen Design and Fabrication
- 5 Results and Discussion
 - 5.1 Homogeneous materials
 - 5.2 Non-homogeneous materials
- 5 Conclusions
- 6 Future Work
- 7 References

Appendix A: Non-destructive testing in education at OSU

Appendix B: Other Specimens Scanned in this Study.

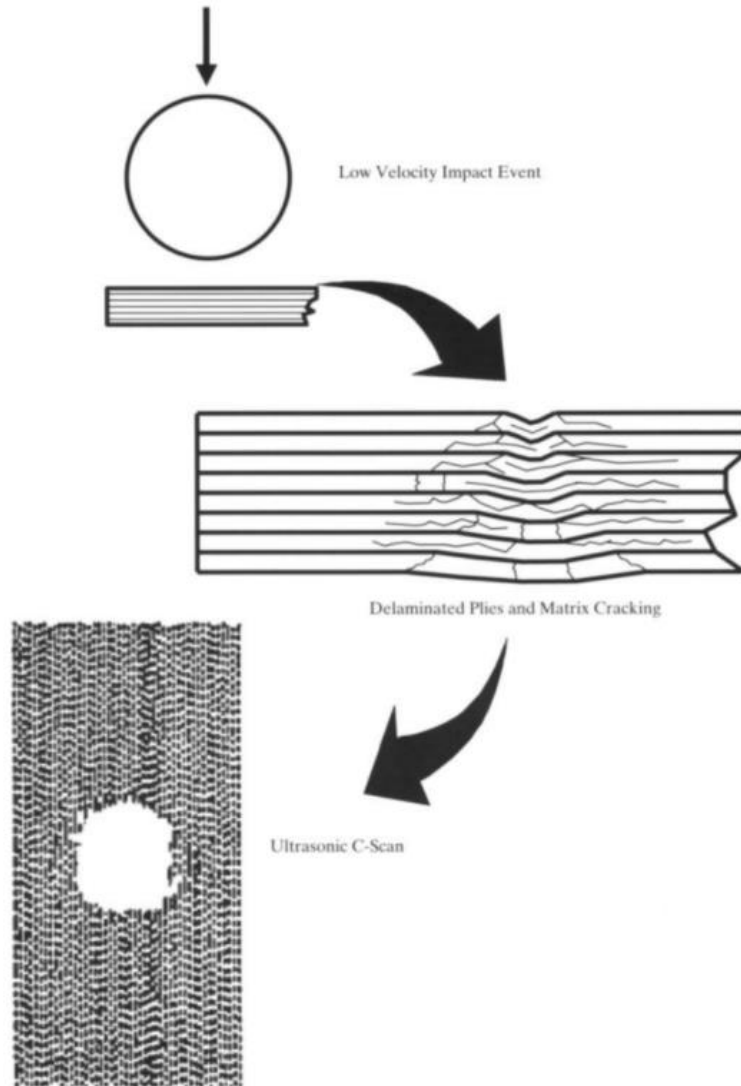
Appendix C: Tables

1 Introduction

A composite material can be defined as a combination of two or more materials that enhance the properties of the structure more than if the materials were used alone [1]. Many modern composites contain two basic components: reinforcement and a matrix. A reinforcement, in the form of short or long fibers and particles, is the element that gives a composite the majority of its tensile or compressive strength and stiffness. In most modern polymers-based composites, the reinforcement is a material consisting of small diameter, typically on the order of microns, high-strength, high-modulus fibers [2]. Common materials used for reinforcements are carbon (graphite), Aramid (Kevlar), and glass. The matrix portion is the binding agent that adheres the reinforcement filaments together and to other objects as well as provides the shear strength to the composite.

Applications and familiarity with composites have grown significantly, as well as their affordability leading to increased production of composites. Testing and development techniques have also been improved and created to allow better composite fabrication and quality assurance (QA). Testing composites through the production process is important to not only understand their limitations, but also to ensure quality in the result. Destructive testing results in the understanding of the extreme limits of the material: where it fails, where it yields, where it bends, where it breaks, as well as how the material can fail. All of this is important to understand how the material can be applied but is not practical to do for each part made. Instead, non-destructive testing (NDT) is one of the foremost testing methods to ensure proper construction and continued integrity throughout the lifecycle of a part. It is also used to assess and classify damaged parts after the part is released to its destination and operations. With modern laminate composites, internal defects from manufacturing processes are also a factor that can weaken the part. For example, layering carbon fiber is a common practice, but introduces the risk of air voids between the layers. These defects reduce the structural integrity and must be identified and quantified to determine damage and eventually to correct faulty manufacturing

processes. Fi 1 shows an example of a damaged composite and how to be able to inspect the subsurface damage is necessary to identify and quantify the damage. Therefore, NDT is very important towards assessing the safety of a composite part.



Fi 1. Composites can be damaged from impacts, and the damage can penetrate beyond the surface, requiring NDT methods for their evaluation.[1]

Several NDT methods are available, many of them apply some form of energy, released and or reflected, to identify potential flaws within the material. X-ray, ultrasound, shearography, and thermography are some of the relevant methods that can identify surface and subsurface flaws. This study presents a Thermal Wave Imaging (TWI)'s experimental setup applied to the identification and classification of defects within homogenous and non-homogenous materials. The technology is based on pulsed wave thermography. Scope of this work is to validate the system when applied to fiber reinforced polymer (FRP) materials, in comparison to homogeneous materials.

2 Background and Literature Review

2.1 Historical Review

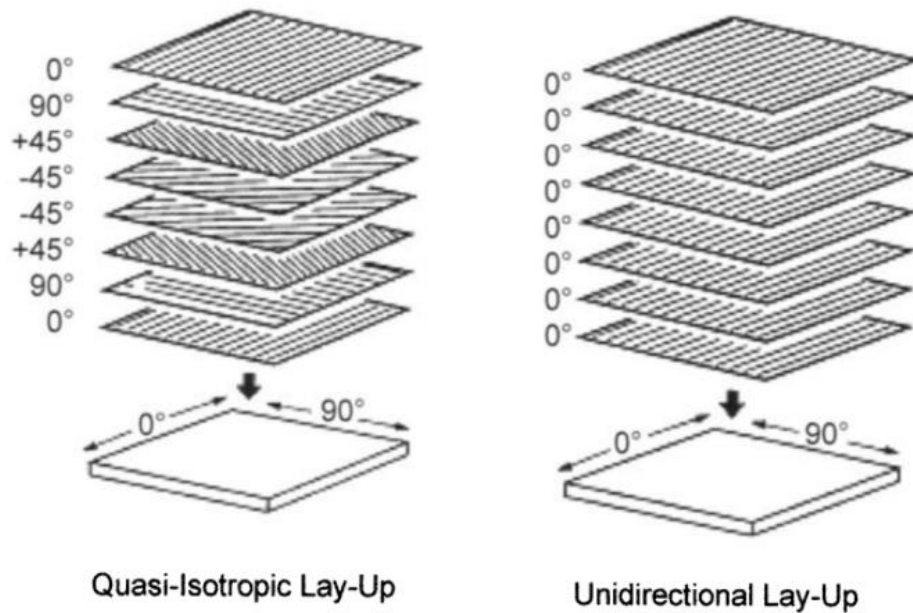
Composite materials are made in a variety of ways. Natural composites, such as bamboo or other woods, have inspired design methods and applications for contemporary FRPs. Wood has different properties when loaded with or against the grain, and the utilization of this can result in improved products' characteristics and performance. Wood is anisotropic, having significantly better mechanical properties in one loading direction than others [3]. It is also non-homogeneous, having a non-uniform structure throughout. The way trees grow causes different densities within which change the mechanical properties. Using layering and lamination, it is possible to maximize the strength and other mechanical characteristics and suppress or mitigate undesirable traits, such as weak points, permanent deformations and the non-uniform structure [2]. Artificial composites were known and applied in weaponry and civil construction since the Roman Empire.

Modern FRPs are typically made in laminates, a series of single plies of the material, with the orientation of each ply specified to have the desired final mechanical properties. This is to ensure that the resulting laminate has the desired mechanical properties in the required directions in reference to the expected loads.

FRPs have a wide array of applications, from use in automobiles, aircraft, and marine vehicles, to insulative or conductive barriers, to civil construction and electronics. The specific strength and stiffness of FRPs can exceed that of other materials that can be used for the same purpose, which can result in significant weight saving for the parts. Composites can also be molded into complex shapes, which can reduce the need for fasteners, as well as reduce the potential for stress concentrations within the part.

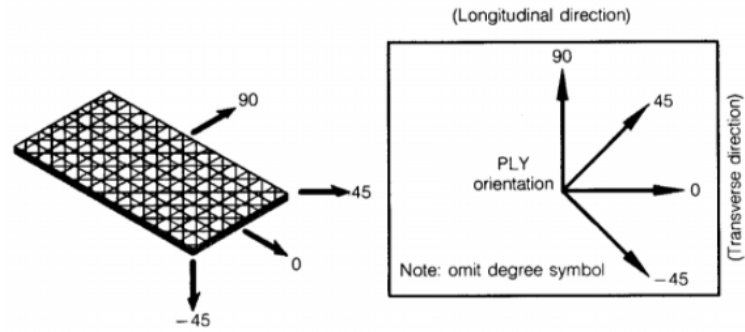
2.2 Fiber Reinforced Polymer Materials

Laminates are generally composed by stacking single plies at different fiber reference angles, in groups or by single ply. Lay up in a direction is typically designed in function of the expected loads on the component. Due to the laminar nature of FRPs, they can be tailored for specific purposes. However, aligning all the fibers in the same direction, for example the 0 degree would not produce an effective part for most applications and is not recommended, because the laminate would be extremely weak in the direction perpendicular to the fiber (in plane) and in shear. As such, composites are laminated with different plies in different orientations. Several plied orientation combinations can give FRPs nearly isotropic, or quasi-isotropic (QI), mechanical properties [2]. An isotropic material has the same structural properties in all directions, such as a metal. An example of a QI laminate is shown in Fi 2.

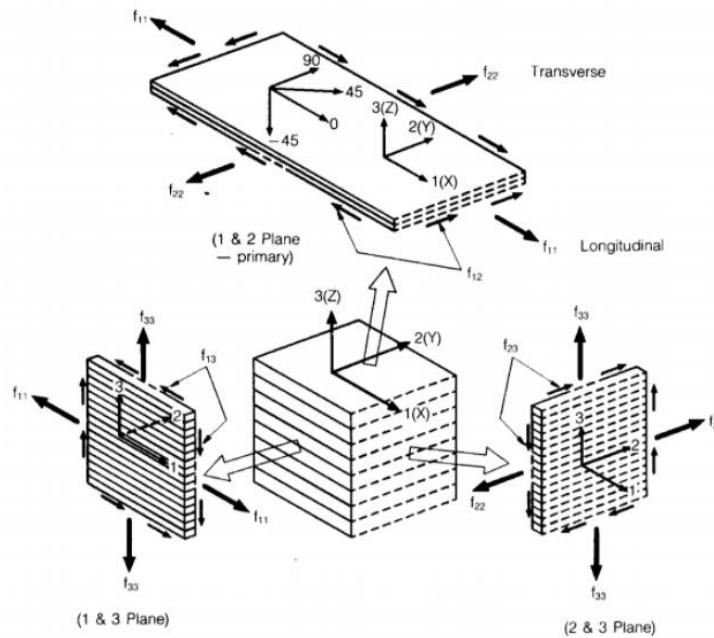


Fi 2. Displays the idea of a quasi-isotropic composite laminate compared to a unidirectional laminate. [1]

Composites are typically anisotropic, having excellent rigidity and strength in the longitudinal directions, but marginal qualities in the transverse direction, unless there are equal plies in the longitudinal and transverse direction, or has a QI layup [2]. The term longitudinal refers to the 0-degree orientation of the fibers within the composite, and transverse being the 90-degree orientation, shown in Fi 3. The orientation and coordinate system of the laminate can be seen in Fi 3. The orientation of the ply and the laminate do not necessarily align, as a ply will be cut according to how it will be laid up in the laminate.



Fi 3. Shows the some of the common angles a ply may be oriented towards and the longitudinal and transverse directions. [2]

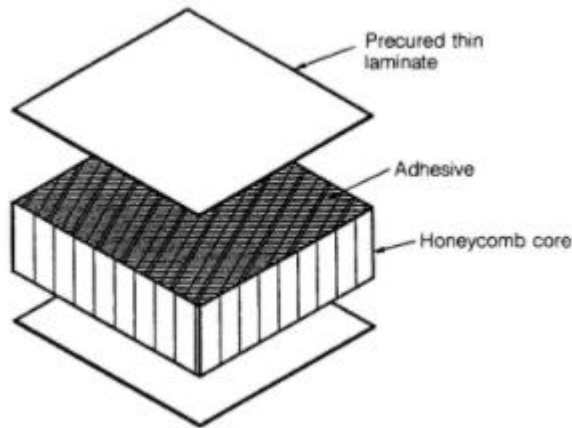


Fi 4. Displays the coordinate system of a composite laminate, including the orientation and x, y, z coordinates. [2]

Composites can be tailored specifically to meet the requirement of the part they are being used for, which allows them to maximize effectiveness while minimizing

weight, waste, and production time [2]. The homogeneous nature of metals makes them an excellent test candidate for creating a baseline for testing FRPs.

In some cases, however, combining composites and metals or other materials creates several desirable properties. A sandwich panel utilizes thin FRP panels that sandwich a core material. The core material could be metal, wood, foam, or other substance with lower density and mechanical properties than the FRP. These panels create high specific stiffness structures ideal for high aspect ratio panels as wings panels, floors panels or hulls and decks for high performance vessels [2]. Honeycomb panels, Fi 5, while useful for such applications, also create unique damage scenarios and can be difficult to ascertain the full extent of the damage until the FRP panel has been removed. NDT offers methods that can allow insight into that damage before removing the panel. However, depending on the materials used, some methods may not be effective.



Fi 5. *The basic honeycomb sandwich panel.* [2]

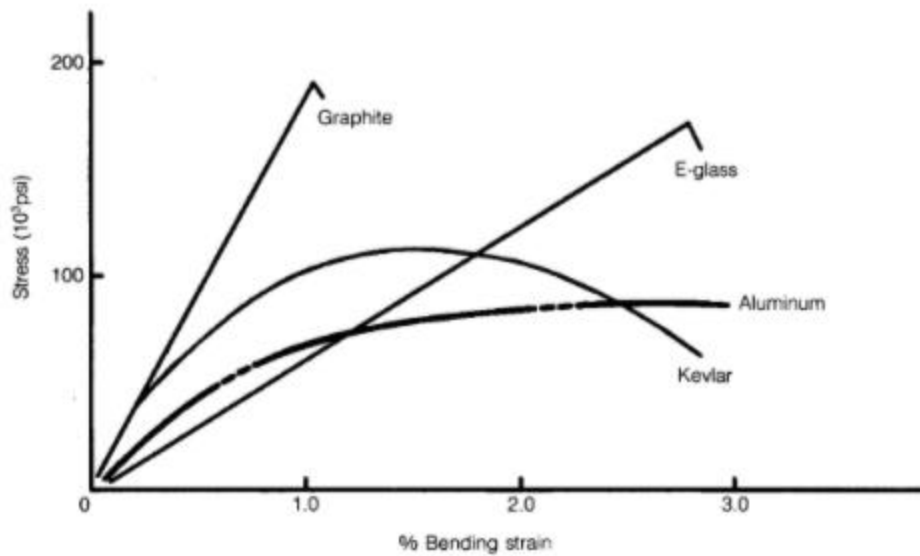
Due to the construction of composites, flaws from production require NDT to ensure quality, and damages incurred during use of a part also need to be inspected.

For structural applications, there are two kinds of fiberglass: E-glass and S-glass. E-glass is the less costly option, and provides the higher strength to weight ratio of the

two, excellent dielectric properties, and great resistance to corrosion, chemicals, and the environment [2].

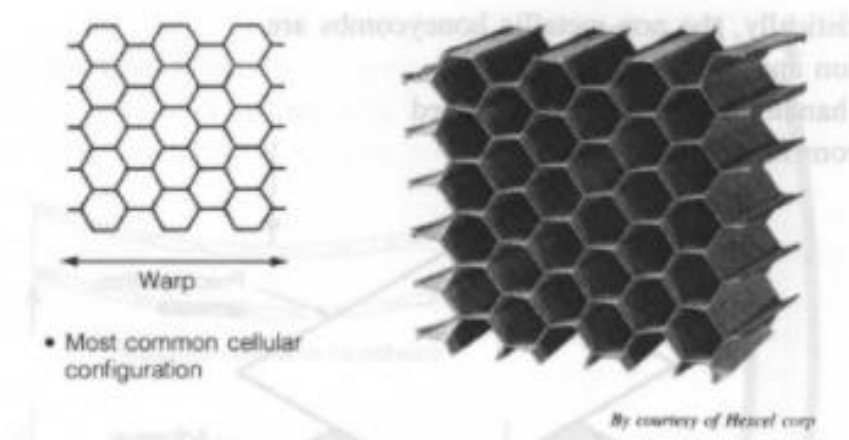
Kevlar, also known as Aramid, is the toughest of the three fiber reinforcement types. Kevlar has very high specific tensile strength but exhibits classically brittle behavior. However, when under tensile and compressive loading in flexural bending, the bending failure is similar to that observed in metals, which helps explain the toughness and impact resistance [2].

Carbon is the last of the common fibers. Carbon has the highest specific stiffness of the three and offers high strength and stiffness to weight ratios, and with proper fiber selection and placement, carbon composites can be stronger and stiffer than metals, at less than half the weight [2]. Fi 6. shows the stress vs. bending strain qualitative curves for the three composites as well as aluminum, which many composites are replacing as structural members.



Fi 6. *The percent bending strain vs stress is very linear for fiberglass and carbon (graphite). Kevlar does not follow this trend, which adds to its toughness. Aluminum is quickly outstripped by carbon and fiberglass, and only surpasses Kevlar at high percentages of bending strain. [2]*

Honeycomb cores can be made from aluminum or Kevlar based paper or polymers depending on the application. Aluminum cores were used in this study, with the hexagonal pattern as shown in Fi 7.



Fi 7. Hexagonal cell pattern for honeycomb core. [2]

The matrix components of composite materials are varied and numerous. They can be separated into two categories: thermoplastics and thermosets. Thermoplastics have better shelf life, short processing cycles, and excellent strain capabilities, but are very viscous when not at processing temperatures, making drapability difficult [2]. Thermoset matrices are used more as they are reactive, allow for better wet out of fibers and good drapability, and can achieve high strength, high stiffness by crosslinking in the polymer networks [2]. Table 3 in Appendix C displays a list of thermosetting matrices and thermoplastic matrices.

2.3 Damage Concepts in FRP

As with any produced part, damage from manufacturing or use can occur. In FRPs, damage is classified as negligible, repairable, or necessitating replacement. Most damage comes from manufacturing anomalies, mishandling, or environmental factors. Any sort of hole, crack, scratch, delamination, or foreign bodies inside or that is not part of the design is damage.

Negligible damage does not affect the structural integrity of the part or assembly. This damage can be permitted to exist as is or can be corrected with a

simple procedure This sort of damage is usually surface nicks or scratches. Repairable damage has two subcategories: patching repairs and insertion repairs. Patching adheres a patch to undamaged portions of the composite and covers the damaged section and is designed to restore full load-carrying characteristics. Insertion repairs are more intrusive, requiring the damaged portion to be cut out and a new portion inserted. This type of repair is used when a damaged section is relatively long, with complex shapes, or when interference between the repair and the surrounding structural member is to be avoided. Lastly, damage necessitating replacement is damage that cannot be repaired or if the damaged part is small enough to make replacement easier than repair. If the part is in a high stress location, and repair would not have a satisfactory margin of safety, replacement is necessitated [2].

Composites respond differently to damage. Kevlar has the highest toughness, and therefore resists impact well. The other reinforcements tend to have various degrees of damage propagation depending on the ply configuration. Damage can propagate more easily through fibers in the same orientation. When the fibers change orientation from one ply to the next, those fibers have cross points between plies. This configuration makes it more difficult for damage to continue into the part. Regardless of the type or extent of damage, many of the damaged portions must go through some NDT to determine the type of damage.

2.4 Testing of Composite Materials

Quality is critical for any manufacturing process. The material must have known operating parameters, such as the tensile and compressive strength, the shear strength, and toughness. These parameters help identify and quantify the limits of the material and can define the conditions under which the material can perform. Initially, when a material is first discovered or produced, the baseline must be set. This involves testing the material to fail, which is referred to as destructive testing.

Destructive testing, in tensile loading for example, applies loads to the material sample and generally increases that load until failure. This test gives an indication of the elastic modulus and the tensile strength limits of the material. However, once these maximum limits and fail loads have been identified, the material can be put into production for specific applications. However, testing the material to fail when it has been made for production is counterproductive. Rather a method of testing or inspecting the product to ensure that it has no defects, or it has been produced as required is sometimes necessary.

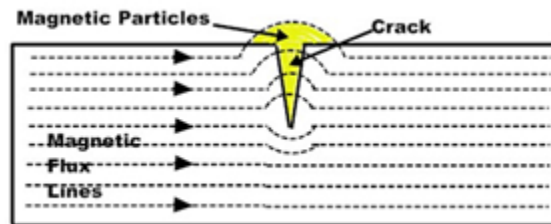
There are a few other types of testing that composites can undergo. Development testing is used to further characterize the materials and processing techniques with those materials. Qualification testing is a subset of destructive testing where a sample part is full-scale tested destructively to qualify for use. Acceptance testing utilizes loads at or beneath the design loads to ensure the structure can perform to specifications. It is performed similarly to destructive testing but does not continue to failure.

NDT technology can inspect components without causing damages, the part can be tested for defects, flaws, or other indications that the part will be unable to perform as required. It is often used in conjunction with the above methods.

2.5 Non-Destructive Testing

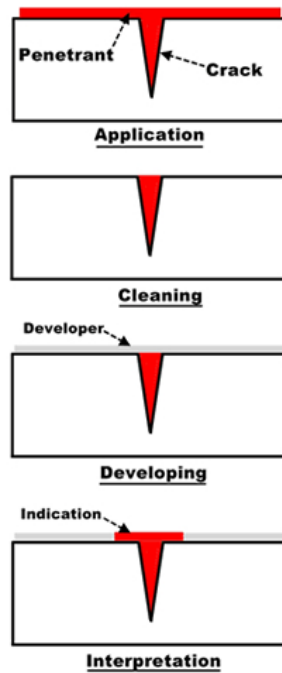
While visual inspection is the easiest, and oldest method, many of the issues with composites are not visible to the eye thus other methods such as Eddy-current, penetrant inspection, shearography, and thermography are applied. Sound was used as another method of indirectly observing the structure of a material. Blacksmiths and other metal workers would listen to the tone their product produced to ascertain whether it was complete or flawed [4]. Around WWII, technology began progressing rapidly, requiring new methods for inspection and more precise materials. The idea of NDT began to grow, and as a result many methods of NDT are now available.

According to the American Society for Nondestructive Testing, the most common methods are magnetic particle testing (MT), liquid penetrant inspection (PT), radiographic testing (RT), ultrasonic testing (UT), electromagnetic testing (ET), and visual testing (VT). MT uses magnetic particles to detect near surface defects with magnetic fields. The particles will coalesce around where the discontinuity in the material is, due to the magnetic flux “leaking” out of the material. This type of testing can only be done on ferromagnetic materials [5]. Fi 8 shows how MT is used to identify surface defects.



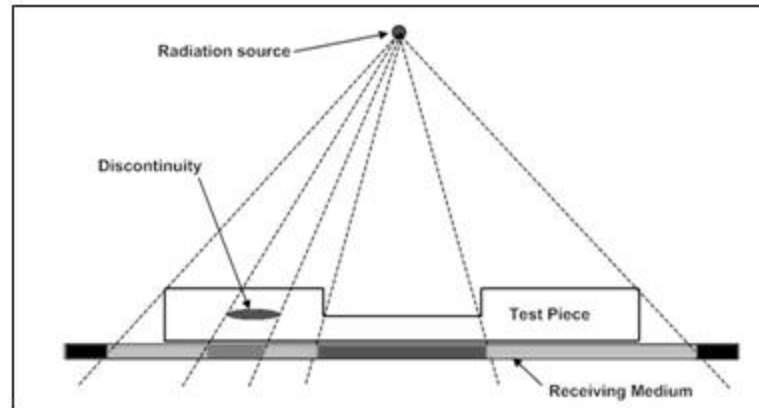
Fi 8. *Damage being assessed using magnetic particles and a magnetic field. The field distorts around the crack, causing the particles to change orientation, indicating a defect. The method is generally applied to metallic materials. [5]*

Liquid penetrant testing has been a common practice, with early applications using oil and a light-colored powder for the detection of defects. Modern applications will use fluorescent penetrants that show up well under ultraviolet light. Dipping the part into the penetrant and letting the penetrant seep into the surface defects, then removing the part and wiping away the excess penetrant allows the cracks and flaws in the part to be highlighted by the penetrant that seeped in [5]. Fi 9 details the general principle of PT, using the penetrant to identify surface defects.



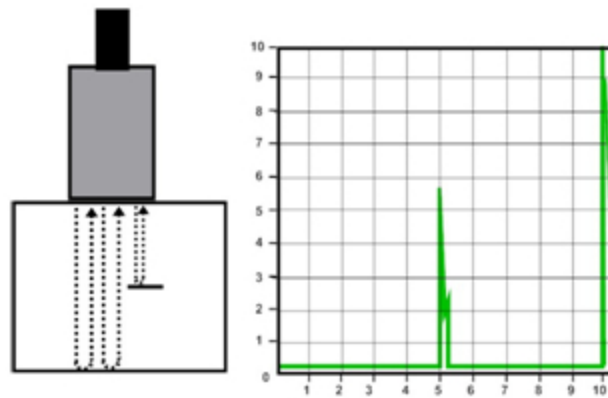
. Fi 9. Penetrant is applied over surface defect, excess penetrant is removed, part is left to sit, usually with a developing substance being applied, and finally the penetrant displays where and the shape of the defect. [5].

RT uses radiation to create an image of the material, passing radiation through the sample onto a film, which then develops an image of the structure of the material. Darker spots on the film indicate where more radiation has penetrated the material, which then indicates a thinner section or internal void, as shown in Fi 10 [5].



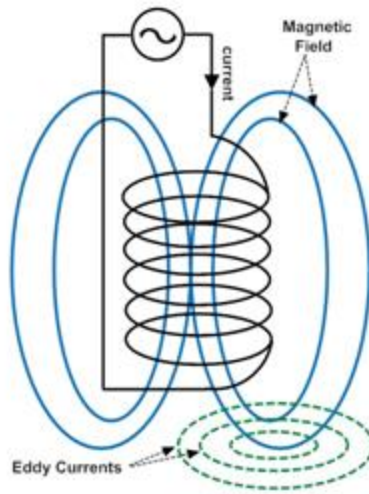
Fi 10. Operating under the same principles as a medical X-ray, radiation bombards the part, and where defects create a more developed spot on the receiving medium. [5]

UT utilizes soundwaves to form an image of the subsurface structure. Ultra-high frequency soundwaves are introduced to the material, and the reflections of that sound are recorded as indicated in Fi 11. Any deviations from the standard material matrix will register a different reflected sound, and thereby produce an indication on the testing display [5]. While this method is versatile, and able to be used in the field, it is also selective in its applications. Thin, clothlike, or coarse materials tend to be difficult to analyze with UT [7].

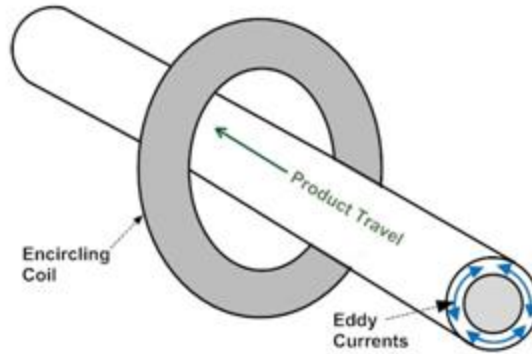


Fi 11. A simple representation of ultrasonic scanning, the image on the left depicting a transducer passing over the surface of a part, and the right showing an output graph of the part, where peaks would indicate defect location. [5]

ET encompasses a few different testing methods, and does include MT, though because of its widespread use, MT is considered a separate test. Eddy current, alternating current field measurement, and remote field testing are the other methods of ET. Each of these methods requires an induced current or magnetic field into a conductive part, as Fi 12 illustrates [5].



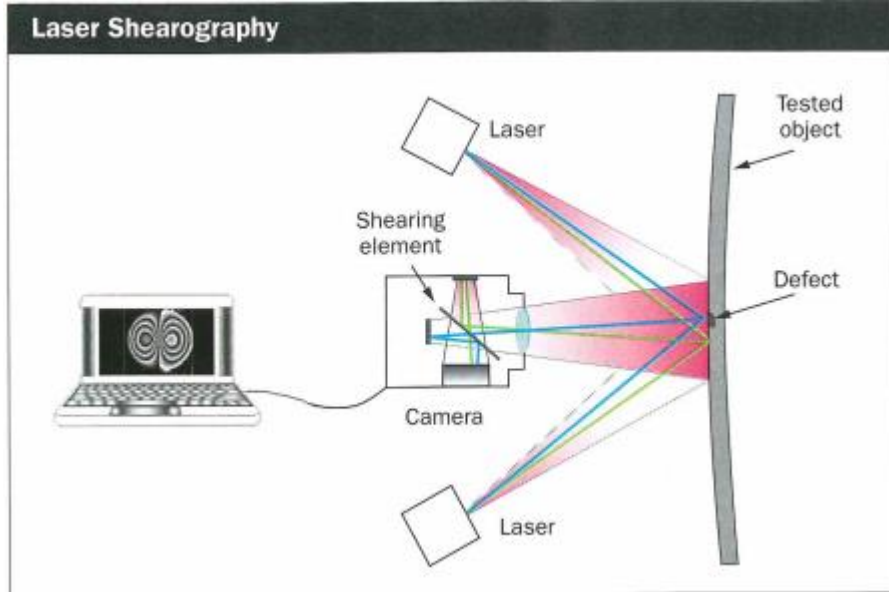
(a)



(b)

Fi 12. *Different methods of electrical testing. Image (a) shows how Eddy-current testing generates eddy currents, and (b) shows how a part may be passed through an Eddy-current setup.* [5]

Laser Shearography (LS), is a non-contact optical testing method that measures nanometric changes in the tested part's surface [8]. Small stress loads are applied to the part while a laser illuminates the surface; the stress field causes geometrical changes to the surface, with internal defects causing changes that differ from the surrounding area. Fi 13 shows a shearography setup.



Fi 13. *Basic shearography setup.* [8]

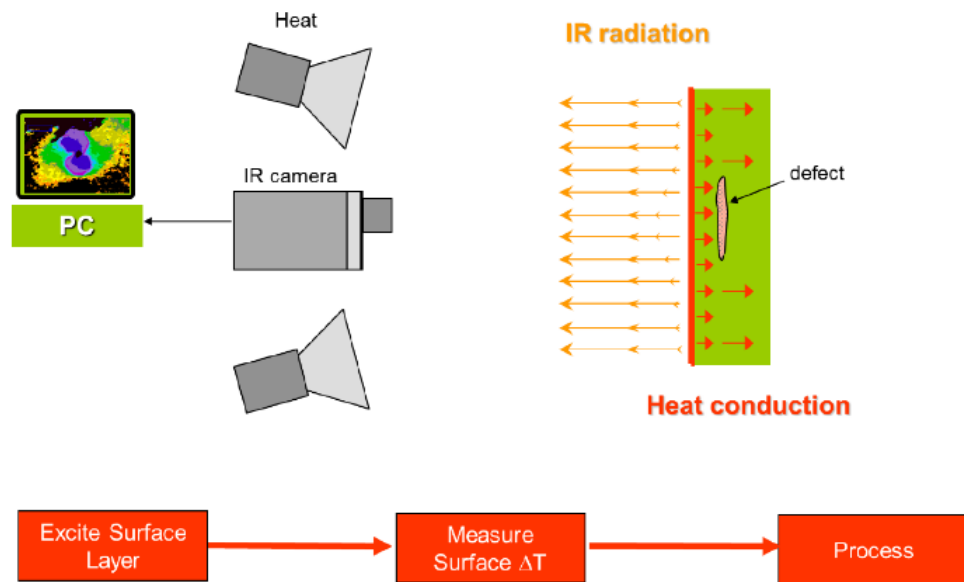
3 Pulsed Wave Thermography

3.1 Thermography Principles and Theory

Thermography, or thermal/infrared testing, maps the surface temperature as heat flows through, to or from the material. An infrared camera is able to record the wavelength of light radiating from the material's surface. Thermal imaging can identify corrosion damage, delamination, disbonding, voids, and inclusions among other detrimental conditions. This study focuses on pulsed thermography. A pulse of heat is applied to the surface of the component to thermally excite the surface of a material and record the surface heat radiation as the heat conducts through the material.

The technology is a relatively new development to the NDT field. While thermography has been used in NDT for a longer time, the application of a light or other heat source to flash and excite the surface of a material has been developed more recently.

Pulsed thermography, based on identifying how the heat disperses through the material, aims to identify the location, depth, size, and shape of defects. A pulse of light is applied to excite the surface of the material as opposed to a constant heat source gradually heating the material. The TWI system, acquired for the Applied Mechanics and Composites Technologies Laboratory at MIME, includes two professional lights with a high flash wattage, and two power supplies with variable power output for different initial excitation of the material. An infrared camera records the radiation heat transfer through the material. An infrared camera records the radiation heat transfer through the material. Fi 14 shows the TWI setup and the basic scan process.



Fi 14. *The simplified version of the TWI setup and the basic function of pulsed wave thermography.* Courtesy of TWI.

As shown, the two flash bulbs excite the surface of the sample, heating it above the background ambient conditions. As the heat conducts through the material, the surface change in temperature is captured by the IR camera. Since defects impede the heat from conducting through the material, the temperatures over a defect will remain warmer, and therefore radiate more heat back to the camera,

The set up used in this study, as defined by Thermal Wave Imaging (TWI), is a custom system using the EV1 Infrared Camera. The system, based on a custom post processing software called Virtuoso, allows for a larger area to be scanned at one time. The supplied IR camera is a 30 Hz camera, which can record images up to that limit. Some materials, namely metals, are able to conduct heat at a rate the camera cannot record well.

Another limitation with the system is the difficulty scanning insulative materials, which can be explained with the emissivity ratio. The emissivity ratio (ER), defined as:

$$E = \frac{\epsilon_{flaw}}{\epsilon_{host}},$$

where

$$e = \sqrt{k\rho c},$$

and k is the thermal conductivity, ρ is the density, and c is the specific heat of the material. This ratio limits the emissivity of the defect to be different than that of the material, otherwise the IR camera will interpret the radiation from the defect the same as the material. As the ratio approaches 1, the system will begin to interpret defects as part of the surrounding material, because the emissivities are similar.

Thermography itself has limitations on the sizes of the defects it can detect. The aspect ratio of the defect limits the size of the defect to be larger than the depth it is within the material. The aspect ratio (AR) is expressed as:

$$AR = \frac{\text{flaw diameter}}{\text{flaw depth}}$$

The threshold of the AR is also 1, as ratios approaching this value require signal processing to detect, and ratios less than 1 would indicate the defect is likely not detectable.

3.2 Virtuoso Software

The Virtuoso software is TWI's proprietary software that utilizes thermal signal reconstruction to analyze the capture from the infrared camera. On a general level, the software works by analyzing the pixel intensity and comparing it to the surrounding pixels. The camera picks up the heat radiated from the surface of the material, which is converted to pixels in the software. Some automation is used to identify the region of interest and deciding the exposure level to display the resulting capture video.

Once the capture video has been processed and loaded, Virtuoso will produce graphs of any selected pixel group, on the plane of the sample surface, of the intensity against time for the duration of the capture. Profile graphs are generated showing the intensity against the pixel number and the location of high intensity locations in the video screen.

Virtuoso utilizes the single pixel approach. This approach utilizes the one-dimensional thermal diffusion equation for the appropriate boundary and initial conditions [9]. For flash or pulsed thermography, the simplest case is an infinitely thick, defect free sample heated instantly by a uniform source. The solution for this case comparing the temperature to the pre-flash temperature is:

$$\Delta T(t) = \frac{Q}{e\sqrt{\pi t}}$$

where Q is absorbed energy per unit area and e is the thermal effusivity of the material, which is defined as:

$$e = \sqrt{k\rho C}$$

where k is the thermal conductivity, ρ is the density, and C is the heat capacity of the material.

For more realistic modeling with a finite slab thickness, L , the solution equation is:

$$\Delta T(t) = \frac{Q}{\rho CL} \left[1 + 2 \sum_{n=1}^{\infty} e^{-\left(\frac{\alpha n^2 \pi^2 t}{L^2}\right)} \right]$$

which behaves similarly to the natural log of the simple solution until a time, t^* , where it deviates from straight line behavior. This time can be determined by the equation:

$$t^* = \frac{L^2}{\pi \alpha}$$

where α is the thermal diffusivity. This equation can also be used to determine the other parameters if t^* is known or measured. t^* is important as it can be used to determine defect depth or sample thickness.

Utilizing the equations above, Virtuoso performs Thermographic Signal Reconstruction (TSR), TWI's patented method for processing and interpreting active thermography data by creating a noise free representation of each pixel, based on automated analysis of diffusion behavior [8]. The data for the pixels in each capture image is converted into the logarithmic domain, then a least squares regression fit is performed to create a polynomial series expression of the time-temperature data for a given pixel. The purpose for curve fitting is filtering noise through the conversions, allowing for improved signal-to-noise characteristics when the polynomial expression is converted back to the time domain [9].

The graphs produced shows the time versus intensity, which shows t^* of defects as well as the time for the heat to conduct to the back wall, which allows the calculation of depth and thickness of defects and material, respectively. The other graph shows the intensity profile, which allows for the location of the defects on the plane of the material to be identified.

3.3 General Testing Procedure

Testing of this system and of the samples is organized into three stages: 1) Material selection, 2) Scanning, and 3) Analysis. Material selection has been discussed and can be summarized by determining the systems capabilities to identify capture time, which defines thickness, and the conductivity of the material. Scanning involves placing the sample within the scope of the camera and running the scan. During the scan, it is advisable to not disturb the camera or the sample, as this will yield bad data. Once the scan is complete, the processing phase automatically begins. The software is programmed to measure the pixels for their color, which is indicative of the radiated heat, and thereby recording how the heat passed through the sample. When the software is complete, the analysis of the scan can be done. The processing will allow graphs to be made of the various pixel groups' history, showing how the heat behaved as it moved through, as well as measuring the location and depth of any internal deviations from the normal matrix of the material.

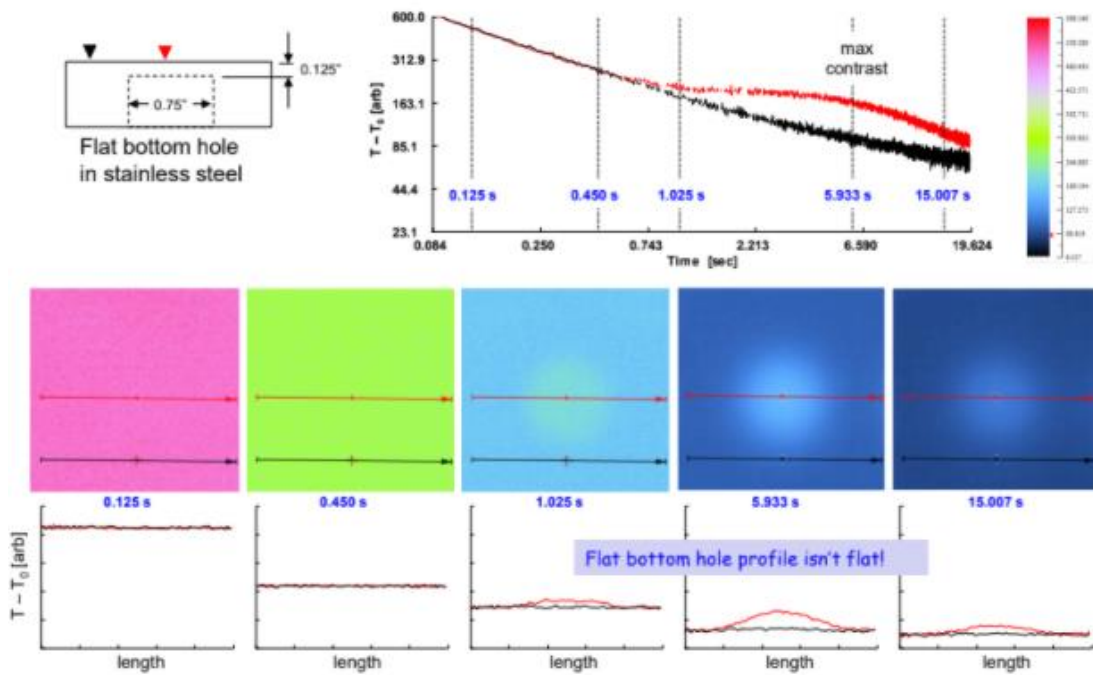
As previously mentioned, the camera is a 30 Hz camera, which limits the range of materials that can be inspected. Metals usually conduct heat quickly, so the required capture time is short, around one second for aluminum allowing around 30 frames captured, which does give the software a limited number of data points for best processing. A camera with a higher frame rate would improve results.

Power is the other constraint. Some materials, such as insulative materials, do not conduct heat well. In some cases, by increasing the power to the flash bulbs, making the flash brighter and more intense, the heat will have enough energy to progress from the surface through the material, revealing the internal struct. More power will also allow the analysis of thicker samples. The flash bulbs can also change the length of flash time from 0.5 to about 30 milliseconds. For this setup, 10 milliseconds were chosen, though a longer flash would have exposed the surface to more heat. Per TWI

specification, the current setup can handle up to ½ inch or 1.27 cm thick samples made of FRP materials and metals.

3.4 Sample of Data Processing and Presentation of Results

The camera records and sends data including the radiated infrared energy from the heated sample to a computer producing a thermal image. The TWI software, Virtuoso, is then able to use that data to plot the radiated heat intensity versus time for a pre-selected set of pixels. By coordinating the frame rate of the camera with the sample's material and power output from the lights, it is possible to see the slope of the radiation energy dissipating through the sample in time. According to TWI, the slope should be $-\frac{1}{2}$ for a normal sample, before reaching the constant value of the background ambient energy as the pulse reaches the far side of the sample, which the camera perceives as the heat transfer going to zero. A normal, unflawed sample will show the negative slope that will drop down until leveling at the background level of heat energy. Fi 15 shows a data acquisition from a hypothetical sample, displaying the normal matrix against the defect.



Fi 15. The image above displays a stainless-steel sample with a hole drilled in it, and the resulting scan, intensity-time graph, and the profile acquired at several times during the scan video. Courtesy of TWI

In Fi 15, the resulting intensity-time graph and profile graphs are the important tools the scan imparts. The intensity-time graph provides depth data about the defect, while the profile graph provides location on the sample. While the video image does show the shape and location as well, the profile graph provides a means to quantify that location.

4 Testing Methods

4.1 Homogenous Materials

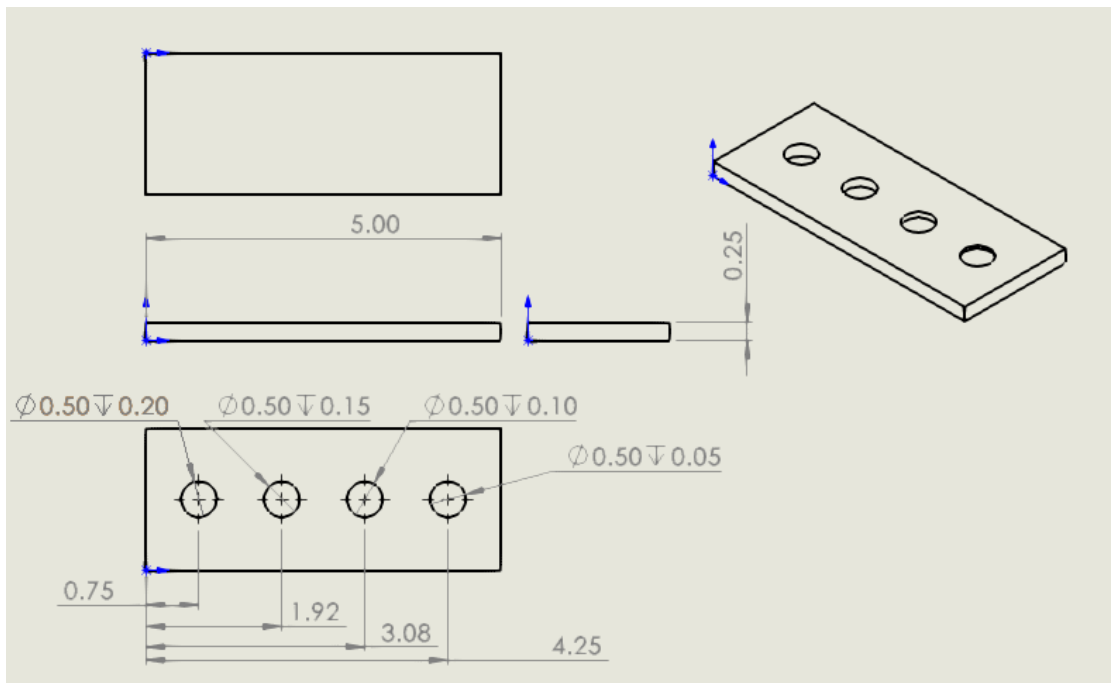
Procedure

The initial tests with this system were performed with aluminum test blocks for their homogenous properties and easy to introduce artificial defects for reference testing. The test blocks were able to be made uniform and have defects of known dimensions machined into them. A few blank samples of aluminum were run through the system to establish a baseline, then test blocks were made to identify defects and test the capabilities of the system.

The aluminum test samples were machined from 2060 Aluminum bar stock. Three test bars were made, each with a different set of defects machined into the back, as shown in Fi 16. A few scans were taken of a blank sample, adjusting various parameters such as the capture time length, the flash power setting, and the polynomial used for curve fitting.

Specimen Design and Fabrication

The aluminum samples, shown in Fi 16, were designed to be small enough to fit within the frame of the camera at a distance that allowed the flash bulbs to uniformly heat the surface. At a distance of approximately 10 inches, the test blocks could be 5 inches long and 2 inches tall. The three aluminum bars were machined to the same length and width, with different size holes to simulate known defects. The first test bar $\frac{1}{8}$ inch holes drilled at different depths. The second had $\frac{1}{4}$ inch holes at different depths, and the last had $\frac{1}{2}$ inch holes at different depths. Fi 16 shows the drawing of the block with $\frac{1}{2}$ inch holes.



Fi 16. *Picture and drawing showing the aluminum sample construction with varying depth holes. Units in inches.*

After a few initial scans, it was determined that the surface of the aluminum samples was too reflective for the given setup. Therefore, the scanned surfaces were painted black to prevent the reflection from disrupting the scan. Some of the paint spattered droplets onto the samples, resulting in bright spots on the scan, which were disregarded.

4.2 Non-Homogeneous Materials

Testing procedure

Testing composites followed the same procedure as the aluminum sample.

Specimen Design and Fabrication

The carbon fiber reinforced polymer (CFRP) panels, shown in Fi 17, used in this study were made to cut hardpoints for the Global Formula Race team at OSU. These panels were made of 120 unidirectional plies following a $[0/\pm 45/90]$ lay-up with a layer of woven carbon fiber on each side. The lay-up had a repeated pattern of 0 degree, +45 and -45 degree, and 90 degree plies that was symmetrically mirrored around the center. The solid plates of carbon are $\frac{1}{2}$ inch, 12.7 mm, thick.



Fi 17. CFRP Panel (With defects marked out after scan).

The composite samples were not manufactured because of the more difficult process needed to obtain materials and fabricate them as well as the limited access to the OSU Composites Lab due to the global pandemic. Also, additional carbon panels from the MFGE 438/538 course were scanned and are shown in Appendix B.

The fiberglass panel, shown in Fi 18, was also obtained for OSU GFR, though the exact composition was unknown. It has similar dimensions to the carbon fiber panels at ½ inch thick.



Fi 18. *Fiberglass Panel.*

The sandwich panels, shown in Fi 19, were constructed with carbon fiber laminates adhered to an aluminum honeycomb core. They had been used to test bending failure prior to scanning.



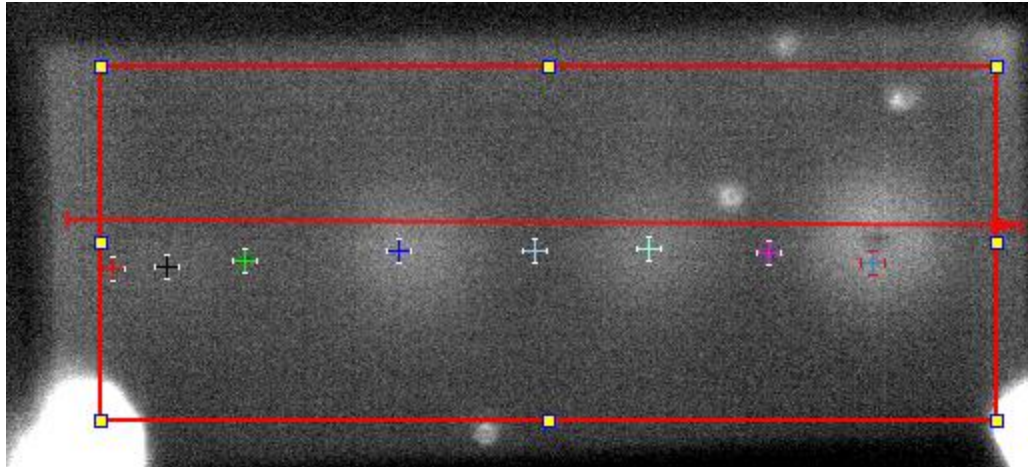
Fi 19. *Sandwich Panel.*

5 Results and Discussion

5.1 Homogenous Materials

Tests on aluminum samples, with a material that was readily available, easy to machine, and homogenous were selected as a basis for procedure and results. Due to the high heat conductivity of aluminum, the flash bulbs radiate to the surface quickly requiring a high capture frame rate to be able to identify defects properly.

Fi 20 shows one aluminum sample with holes drilled at different depths to simulate a controlled defect. The camera was set at 30 frames per second. From left to right the holes are progressively deeper relative to the back of the sample (the side facing away from the camera). The other intense areas on the sample are from the paint used to prevent the aluminum from reflecting the light. The red box is the region of interest (ROI), which Virtuoso uses to heighten the contrast to make the defects more visible. The red line through the middle was made to identify the profile of heat radiation intensity. With clear defects, the profile should display the location of the defects from a reference point. The markers are the points selected for analysis. Each point will generate a line graph for the pixels around it and their progression through the cycle. Fi 21 shows the lines corresponding to the same-colored marker in Fi 20.

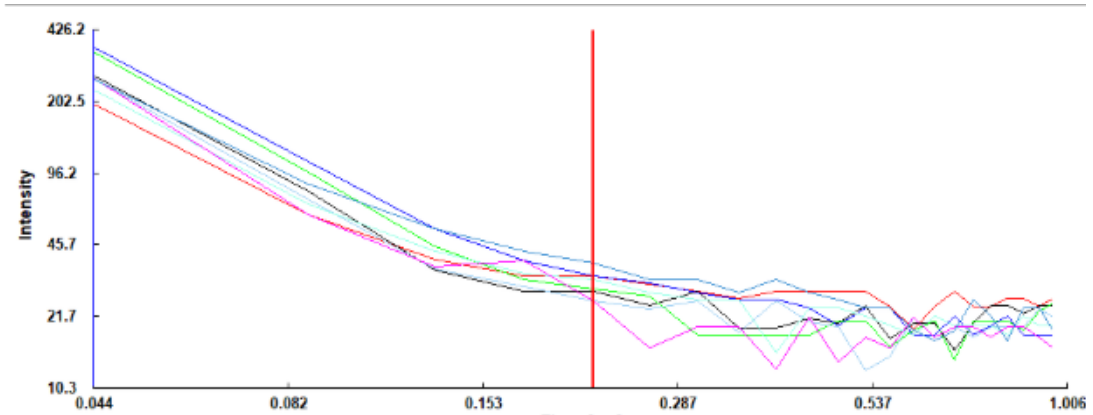


Fi 20 Image of the capture video when the defects were at the highest contrast to the surrounding material. The colored markers correspond to the curves in Fi 21 and the red line corresponds to the profile graph in Fi 22.

In this case, since the defects were large relative to the thickness of the sample, they were easy to detect. As the depth of the hole decreases, the defect becomes more difficult to detect, and harder to observe, as can be seen from the left-most hole, which is barely discernible.

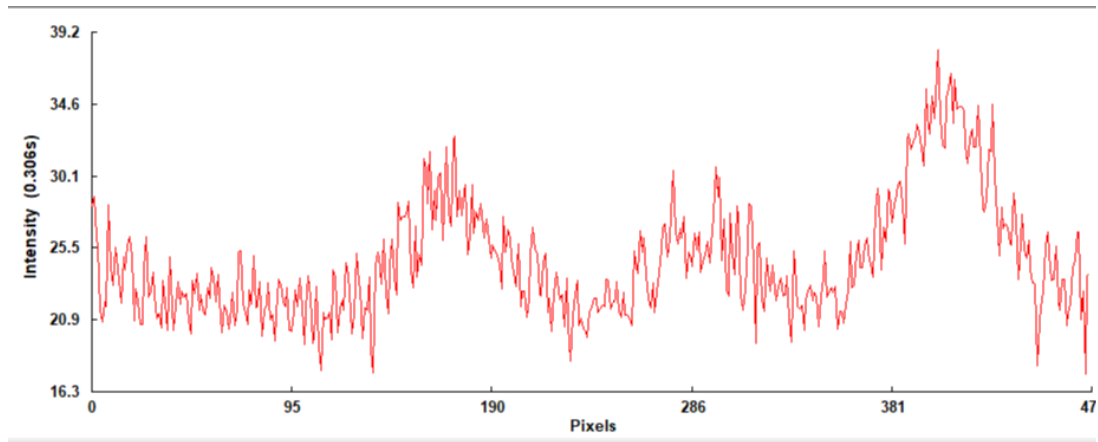
The graph in Fi 21 shows the time-intensity graph of the selected points in Fi 20 as represented by the colored markers on the image. With a defect, the line should begin to level horizontally from that slope, whereas a defect free spot would continue on that slope until the background level of heat radiation is reached, at which point the graph will level horizontally.

The high conduction of aluminum coupled with the sloped edges of the drilled holes offers little difference between the defect and non-defect portions of the sample before background levels are reached. Given that the intensity-time graph is just over one second, the system only captured 30 frames, 10 of which were pre-flash, which results in insufficient data for the software to utilize.



Fi 21. *The intensity-time graph of the sample in Fi 20 showing heat intensity on the y axis and time on the x axis, both in log scale. Due to the speed with which aluminum conducts heat, the camera was not able to detect the defects before the sample cooled to ambient temperature.*

The profile graph, shown in Fi 22, indicates where the defects are in the sample. Each peak in the profile corresponds to the locations with the highest heat radiation on the sample. This is useful in identifying the location of internal defects, by allowing the software to mark the pixels where the defects are, which can then be translated into a physical distance. The profile line in Fi 20 can also be oriented in any direction, so vertical or other distances can be found as well.



Fi 22. *The profile graph of Fi 20. Peaks show highest points of heat intensity.*

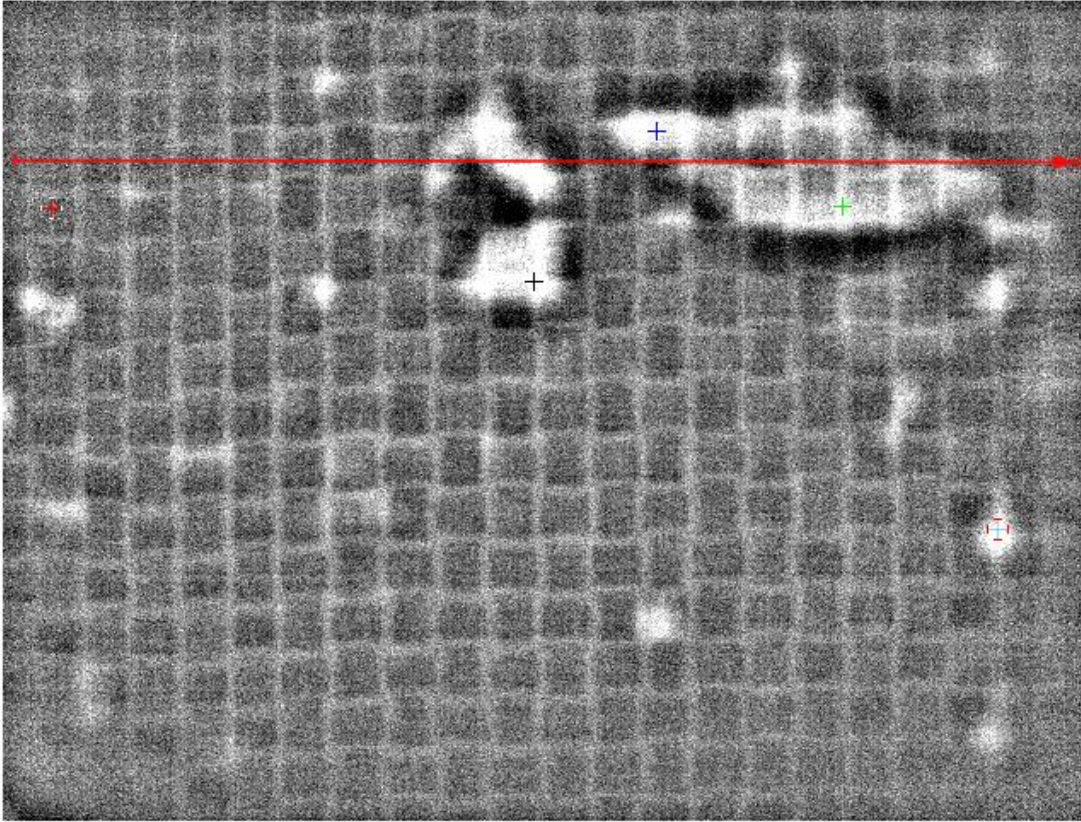
A holes aspect ratio is defined as the ratio of depth over diameter. Aluminum samples with holes with aspect ratios close or smaller than one did not show this amount of detail. For the test bars with $\frac{1}{4}$ inch, and $\frac{1}{8}$ inch holes, the AR becomes one or less than one, meaning the depth is greater than the diameter, making it difficult for the system to detect it.

5.2 Non-Homogenous Materials

Tests on composite samples offered more informative data for a series of factors including the different conduction rates, the different surface finishes, and the nonuniformity of the material.

Carbon Fiber Panel

The carbon fiber panels produced the best results and graphs of this study. Fi 23 displays a scanned section of the carbon fiber panel provided by GFR



Fi 23. *Image displays a section with prominent defects in the carbon fiber sample. The surface layer weave pattern is also visible.*

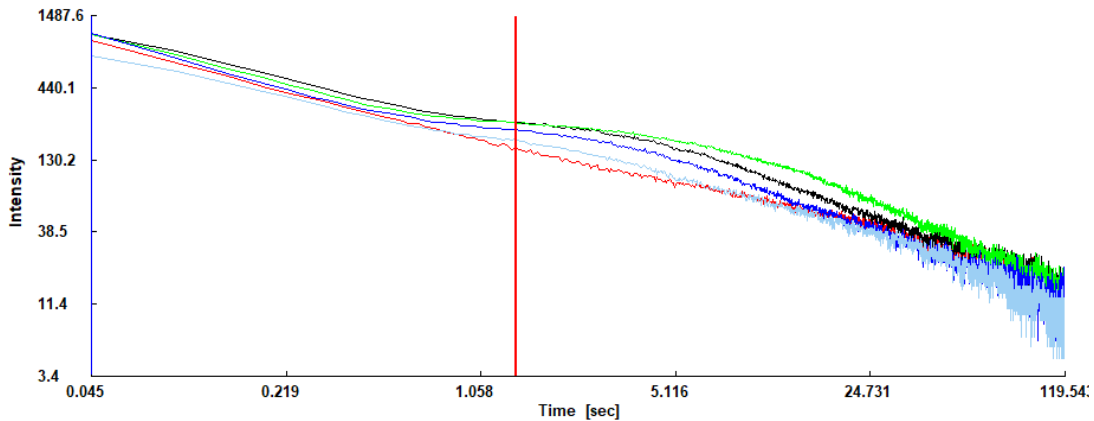
The provided samples had no premade defects, which is why the resulting images have irregular shaped defects. These defects are likely disbanded voids between plies. Defect curves were compared to a defect free area and to the aluminum sample, showing that the carbon fiber panel had better definition around the defects. This resulted in better clarity and definition in the intensity-time graph shown in Fi 20. The graph clearly shows the t^* time for each of the selected defects as compared to the defect free material. Using the green marker and curve as a reference, the defect has a t^* time of about 1.5 seconds, and according to the Virtuoso material library, carbon fiber composites have a thermal diffusivity of $4.167 \text{ E-}7 \text{ [m}^2 \text{ s}^{-1}\text{]}$. Manipulating the t^* equation, the depth of the defect in the material can be found:

$$L^2 = t^* \pi \alpha$$

$$L = 0.0014 \text{ m}$$

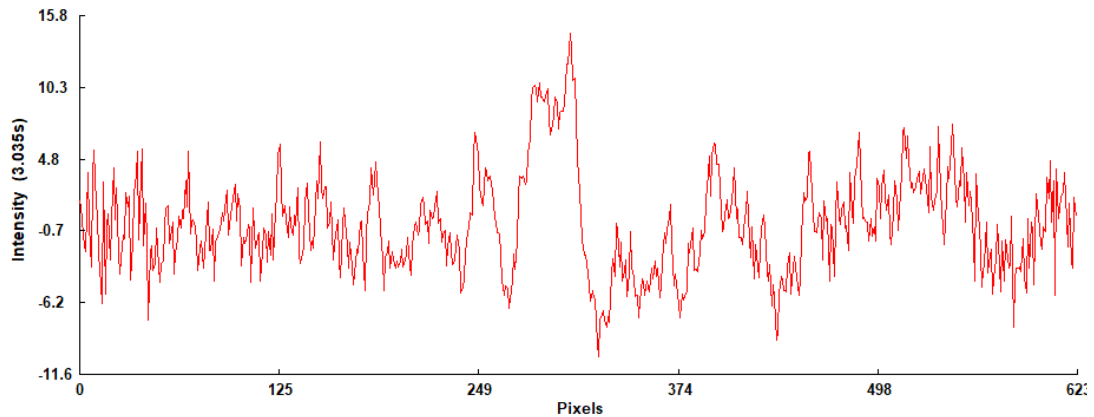
The calculated depth of this defect is 1.4 mm. It is approximate because the capture video is played back on a logarithmic scale, and each frame does not align with an even time integer, as shown on the graph. Also, the diffusivity given in the Virtuoso materials library, which is needed for the t^* equation, is an estimate, as composites differ from one laminate to the next. However, given that the sample was a total of 12.7 mm thick, a defect at a depth of 1.4 mm is plausible.

It is relevant to note from the graph in Fi 24 as compared to the graph of aluminum in Fi 20 is the time scale. The aluminum scan was for just over a second, whereas this scan was for 120 seconds, indicating the difference in the conductive properties of the materials. The fact that the carbon fiber took longer to scan improved the results, as the camera was able to record sufficient data before ambient temperature was approached.



Fi 24. *The intensity-time graph for the carbon fiber panel. The red line shows the defect free area, and each of the others corresponds to a defect.*

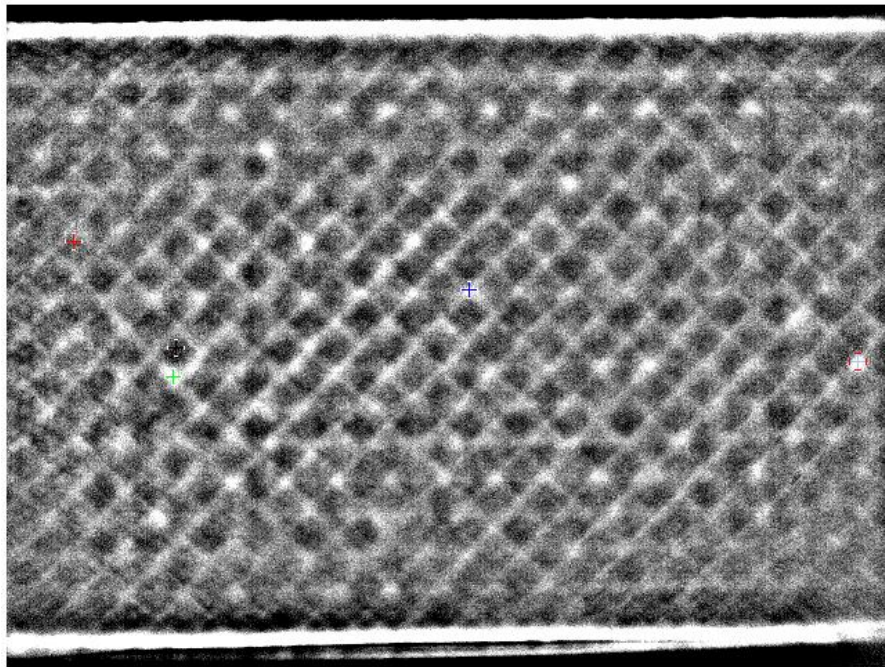
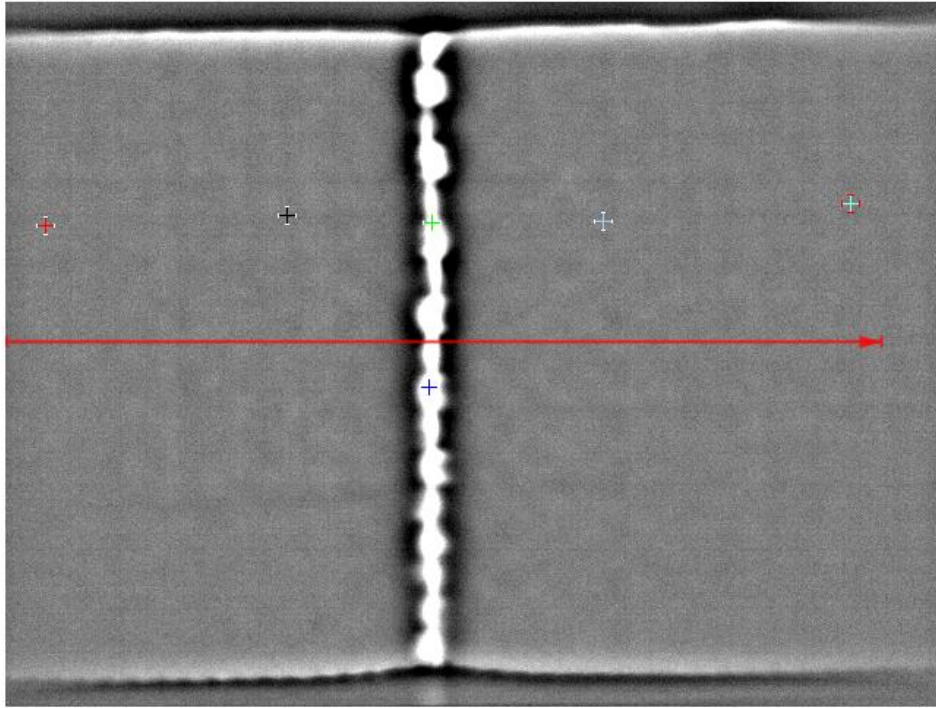
The profile graph of the carbon fiber panel, Fi 25, shows the peaks where the heat intensity is highest. Interestingly, the profile shows the defect towards the center as the most intense, but the larger defect to the left is only marginally registered as expected since the defects are at different depths, and the defect on the left was deeper, resulting in less intense heat in the same frame.



Fi 25. *Profile graph of the carbon fiber panel in Fi 23. Shows the center defect as most intense and the others as only marginal peaks.*

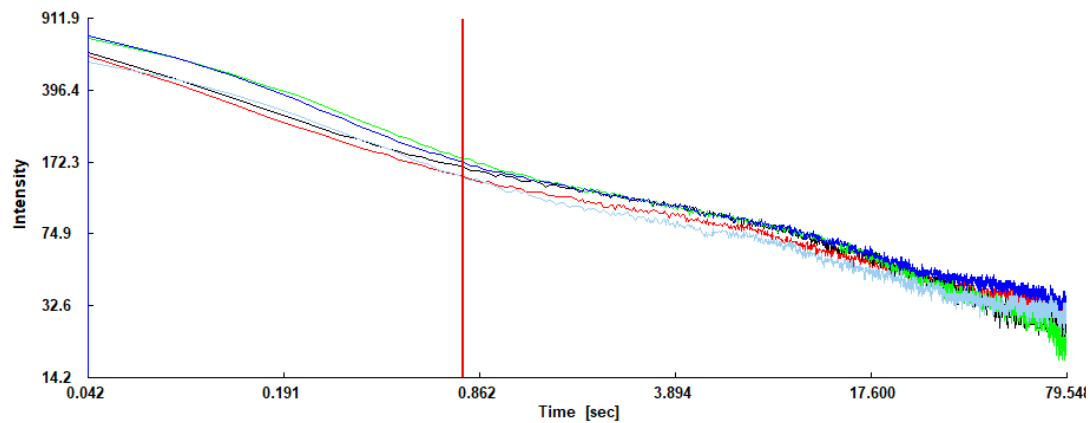
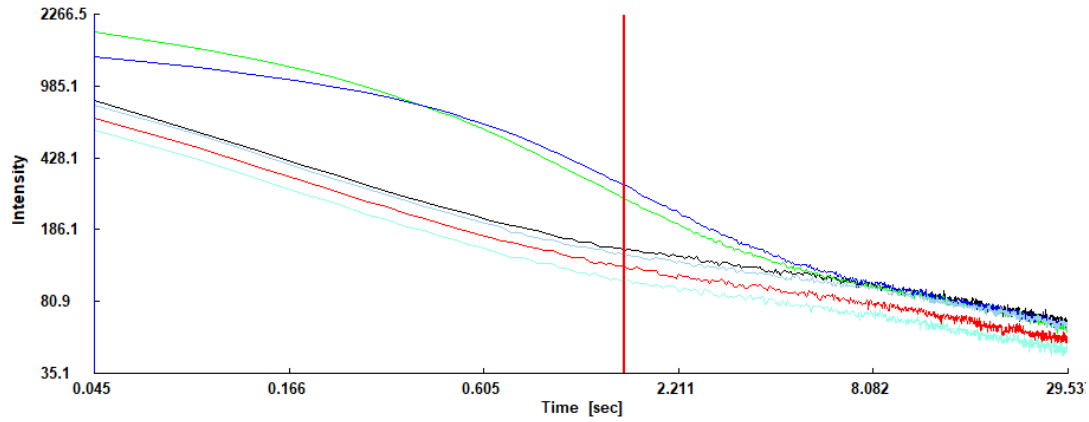
Sandwich Panel

The sandwich panels displayed unique scans. On the front, the scan easily identified the area where the damage occurred. However, the aluminum core allows the heat to conduct extremely quickly through the material and adds a significant convective heat sink for the carbon fiber panels on either side. The metal core is highly heat conductive and extremely thin; thus, the system cannot properly detect the heat conduction through the pattern. Fi 26 a and b show scan images of both sides of the large sandwich panel. Pictures of a sandwich panel in Appendix B.



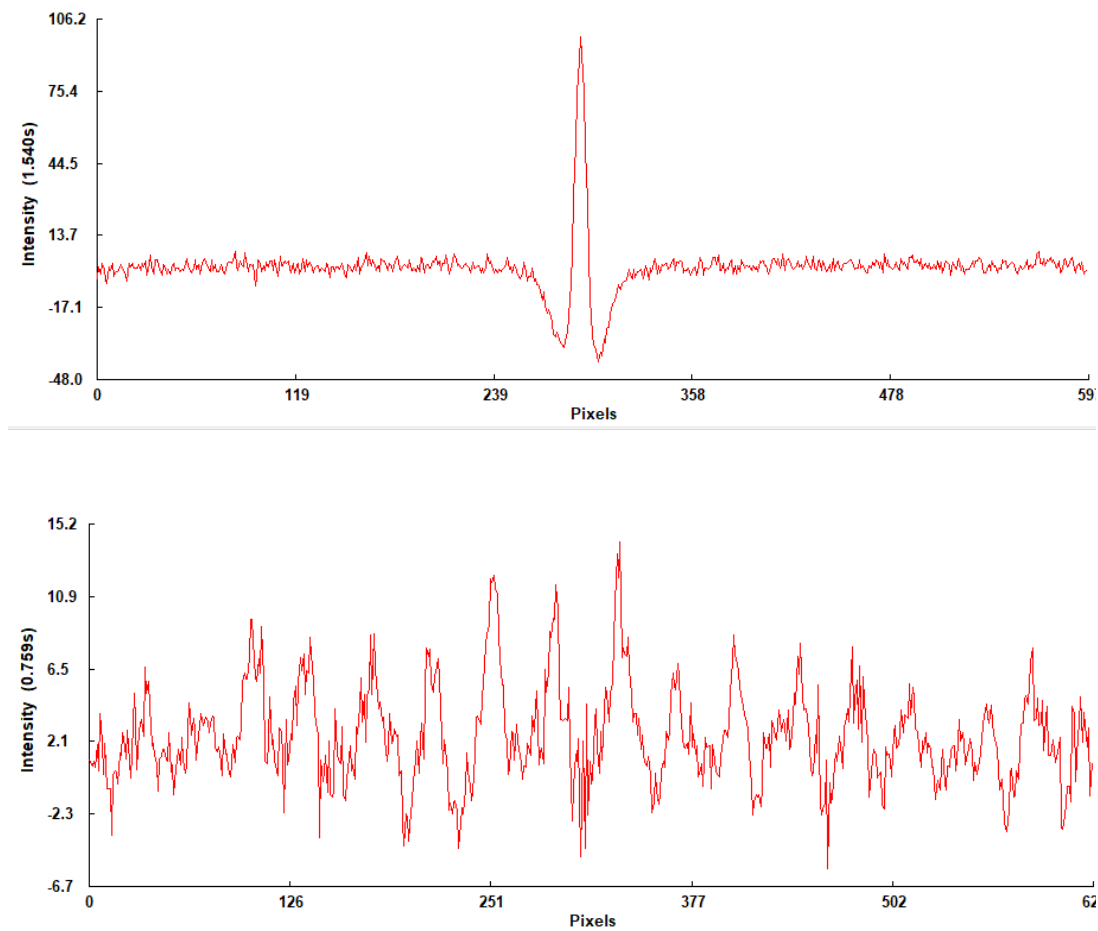
Fi 26 a and b. *Both sides of the large sandwich panel. The front clearly has the bend damage down the center of the frame. The back displays the weave pattern more prominently, but no indication of the damaged section can be shown.*

The graph of the front of the sandwich panel in Fi 27 a and b show the curves associated with the damaged section not following the curves of the surrounding matrix, but rather than begin at the same intensity level, they start higher. This is likely because the damage affected the surface of the material, so instead of conducting normally through, the heat conducts more slowly and therefore begins at a higher intensity since more heat is concentrated there. The back side of the panel follows the same trends to a less pronounced degree, but not showing the same damage. Likely, the aluminum core prevented the system from observing the heat conduction thus failing to show the damage.



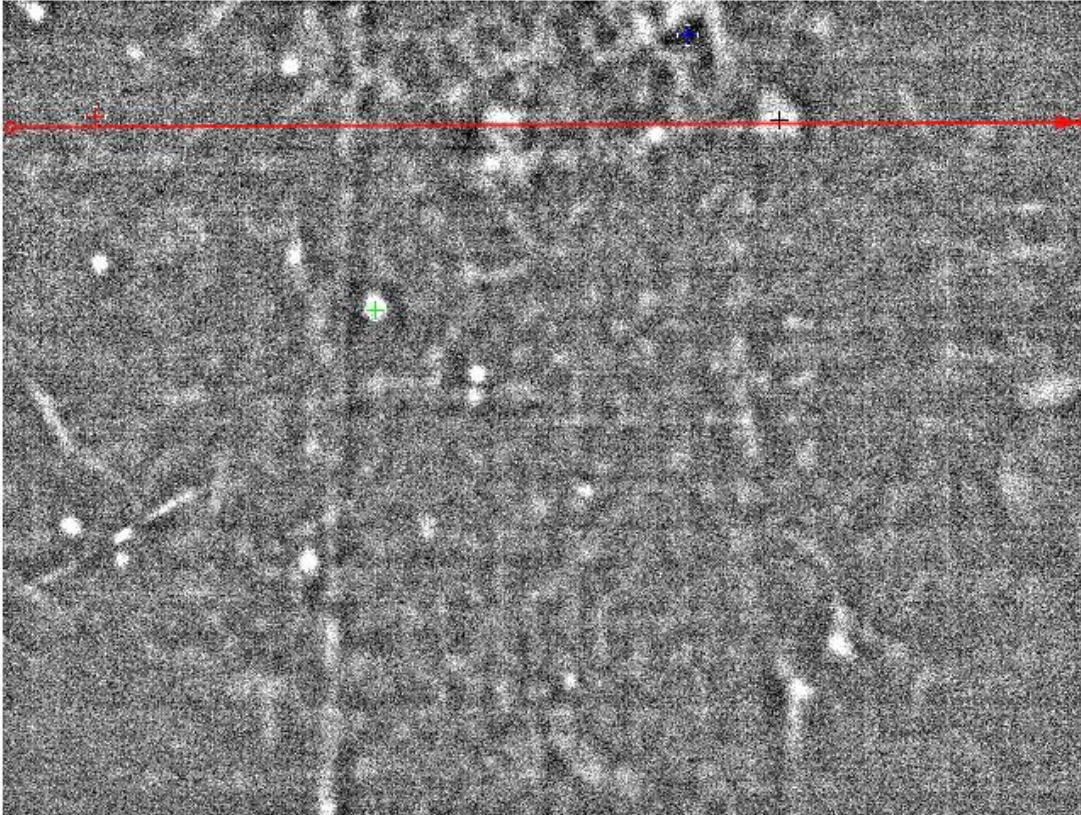
Fi 27 a and b. *The front and back of the sandwich panel scan in Fi 24 a and b, respectively.*

The profile graphs are shown in Fi 28 a and b. The front shows the damaged section very prominently displaying the most intense heat. Where the damaged section transitions to the undamaged section, the profile graph shows less intense heat indicating extremely fast conduction of heat. The back of the panel, Fi 26-b, displays a more typical profile graph, with many local peaks corresponding to cross points in the weave, which have gaps in the fiber in that area, and therefore are less conductive.



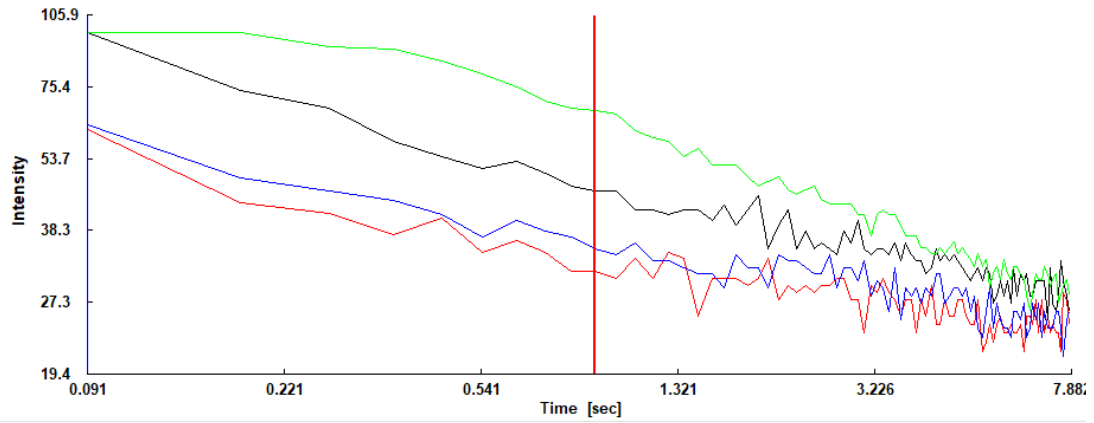
Fi 28 a and b. *The profile graphs of the front and back of the sandwich panel, respectively.*

Lastly, the fiberglass panel was the most challenging material to select system settings (frame-capture rate and power level) that resulted in any usable curve. More interesting, the fiberglass did not show a clear internal structure at all. The majority of what the system was able to detect were likely minute surface flaws. Because of the low thermal conductivity of fiberglass, one order of magnitude less than carbon fiber, no meaningful results were obtained for the characterization of internal defects. The system is not able to heat the surface enough with the current pulse to penetrate through the fiberglass, and therefore cannot read the heat radiation traveling through the sample. The ER of the fiberglass is close to one, meaning that the heat radiation across the surface looks uniform to the system. The spots that do register on the scanned image, shown in Fi 29, indicate that they are surface imperfections, and not within the material.



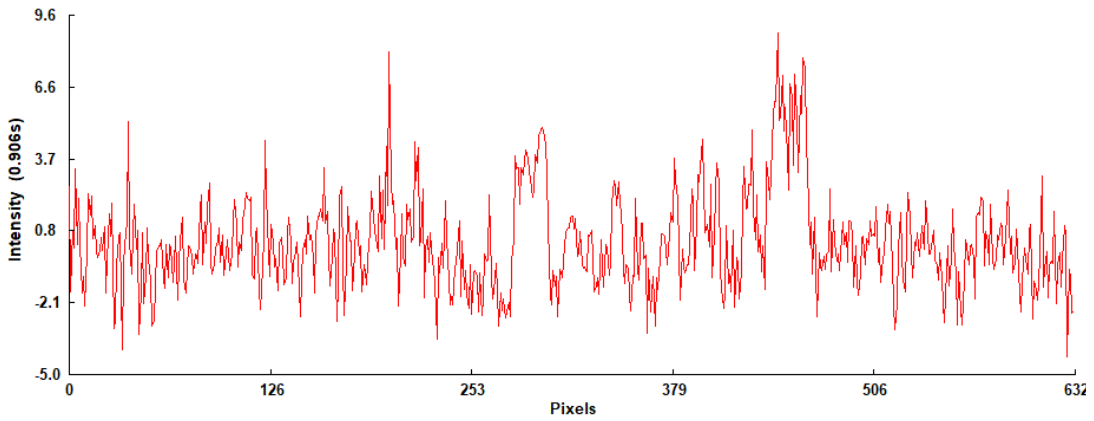
Fi 29 The scan image of a portion of the fiberglass panel. All other scans were similar in composition, or distorted due to different settings.

The time-intensity graph for the scan, shown in Fi 30, is reminiscent of the aluminum scans with noise developing quickly, despite having a scan time of eight seconds. The scan has a multitude of bright points, with no options to select a reference. The selected bright points were the larger points, as many of the smaller points became noisy more quickly, which prevents good analysis of not only the small points, but other points on the graph as well.



Fi 30. *The time-intensity graph of fiberglass.*

Lastly, the profile graph, Fi 31, does show the intensities across the scan, which would reveal the locations of the points the line crosses. The line was placed across the section with the most variation, and the two bright points are shown as the peaks in the profile.



Fi 30. *Profile graph of fiberglass panel.*

6 Conclusions

The system offers good imaging and qualitative analysis of subsurface material defects. Reiterating that the camera does not have a high enough capture rate to be able to identify defects in metals, the entire system is still able to produce visual indications of where defects are within the metal. The system can identify the heat diffusion through the metal, allowing the x-y coordinates of the defects to be defined. However, the graphs are not as informative due to the low capture time that metals would require. Large defects were detected and localized using profile graphs. However, high levels of noise were reported in the graphs due to the high conduction of aluminum.

With FRPs, the system showed good capture and data acquisition with carbon samples, allowing for reliable information about the depth of defects as well as the location and size. Composites sandwich panels showed good results for the carbon portion, but due to the honeycomb metal core, the system was unable to obtain internal structure information due, as in the case of homogeneous aluminum samples, the heat was rapidly dissipated. Tests on fiberglass epoxy panels showed several intense areas across the surface. However, the system was not able to inspect the internal structure, likely due to the higher emissivity and high insulation properties of fiberglass. Results presented highlight the generally good identification of problematic areas that are present in the laminate represented by several surface points of higher intensity. Those results cannot, however, represent features of the internal structure.

7 Future Work

Future tests should involve the more advanced functions of this system. Given that the system performs well with carbon FRPs (CFRPs) more samples should be made to test these functions. A wider selection of pre-processed composites, that is, more CFRP samples with pre-placed defects, should be run through the system to further develop the total limitations of this system, as well as to test accuracy against the known locations. In addition, labs using the technology will teach students to use the system for defect identification and localization on pre-tested parts with specified artificial defects. Comparing these results to results of other systems, such as UT would reveal where the technologies overlap and correlate, and where they differ and how to use the differences to the advantage of the user.

Other projects requiring the use of a NDT system, such as the GFR Chassis, the DBF aircraft or the numerous rocket competitions teams may also be interested in utilizing this system for more specified testing and product confirmation. Many of the parts scanned by these organizations may have more complex geometry, so developing a method for scanning such shapes is another future project.

8 References

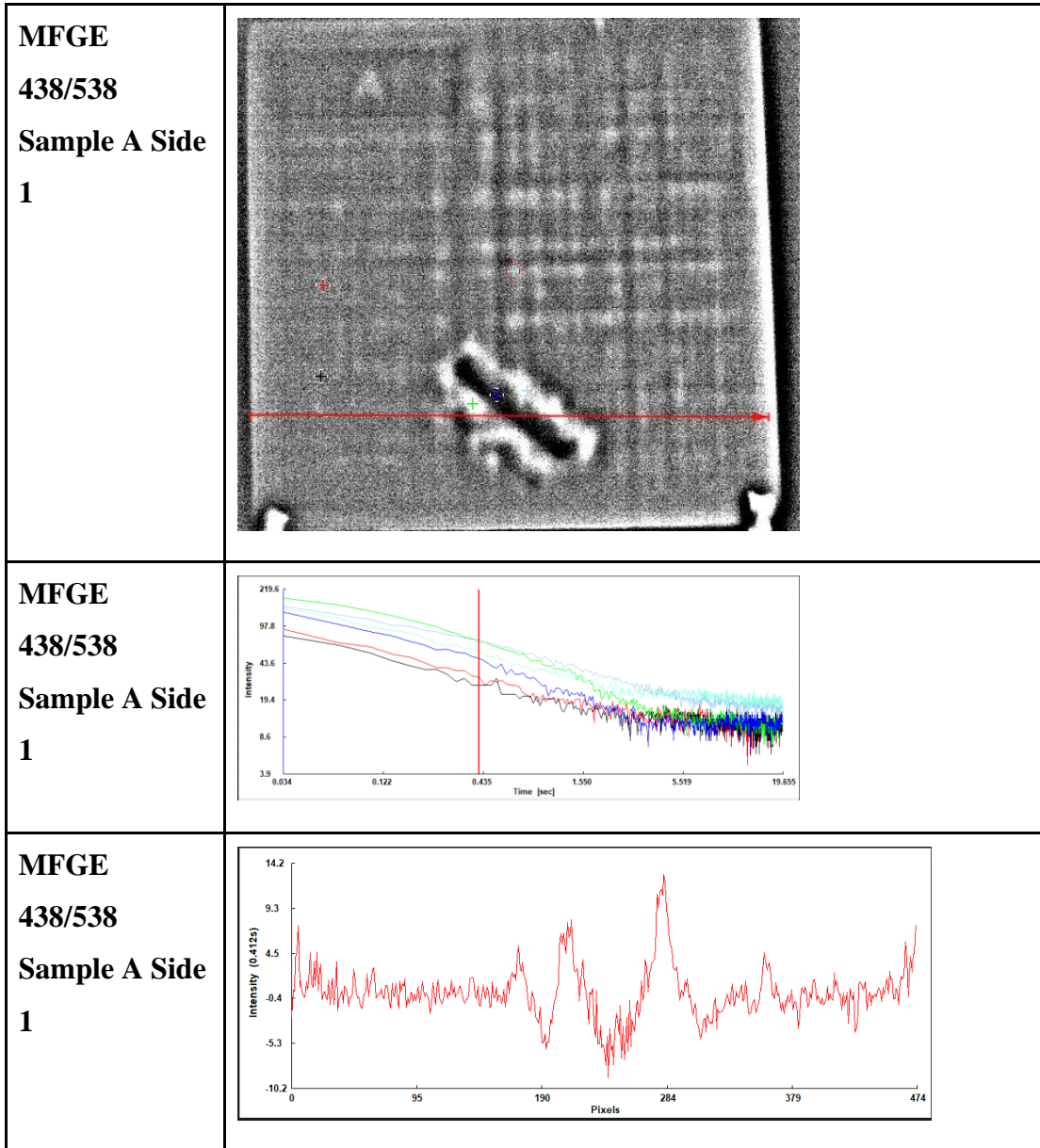
- [1] F.C. Campbell. *Manufacturing Process for Advanced Composites*. Oxford, Elsevier Advanced Technology, 2004.
- [2] Niu, Michael Chun-Yung. *Composite Airframe Structs*. Conmilit Press, 1992.
- [3] Malaga-Toboła, Urszula, et al. “Influence of Wood Anisotropy on Its Mechanical Properties in Relation to the Scale Effect.” *University of Agriculture in Kraków, Balicka 116B, 30149 Kraków, Poland*, International Agrophysics, 2019.
- [4] World Of NDT. “History of Non-Destructive Testing (NDT).” *World Of NDT*, World Of NDT, 16 May 2020, worldofndt.com/history-of-non-destructive-testing/.
- [5] “Introduction to Nondestructive Testing.” American Society for Nondestructive Testing, ASNT, 2019, asnt.org/MajorSiteSections/About/Introduction_to_Nondestructive_Testing.aspx.
- [6] Pfund, Bruce. “Now You See It.” *Professional BoatBuilders*, pp. 26–28.
- [7] “Basic Principles of Ultrasonic Testing.” Introduction to Ultrasonic Testing, NSF-ATE, www.nde-ed.org/EducationResources/CommunityCollege/Ultrasonics/Introduction/description.php.
- [8] Scalvini, Roby. “Shearography in the Expanded Frame.” *Professional BoatBuilders*, pp. 38–44.
- [9] TWI Virtuoso User Guide

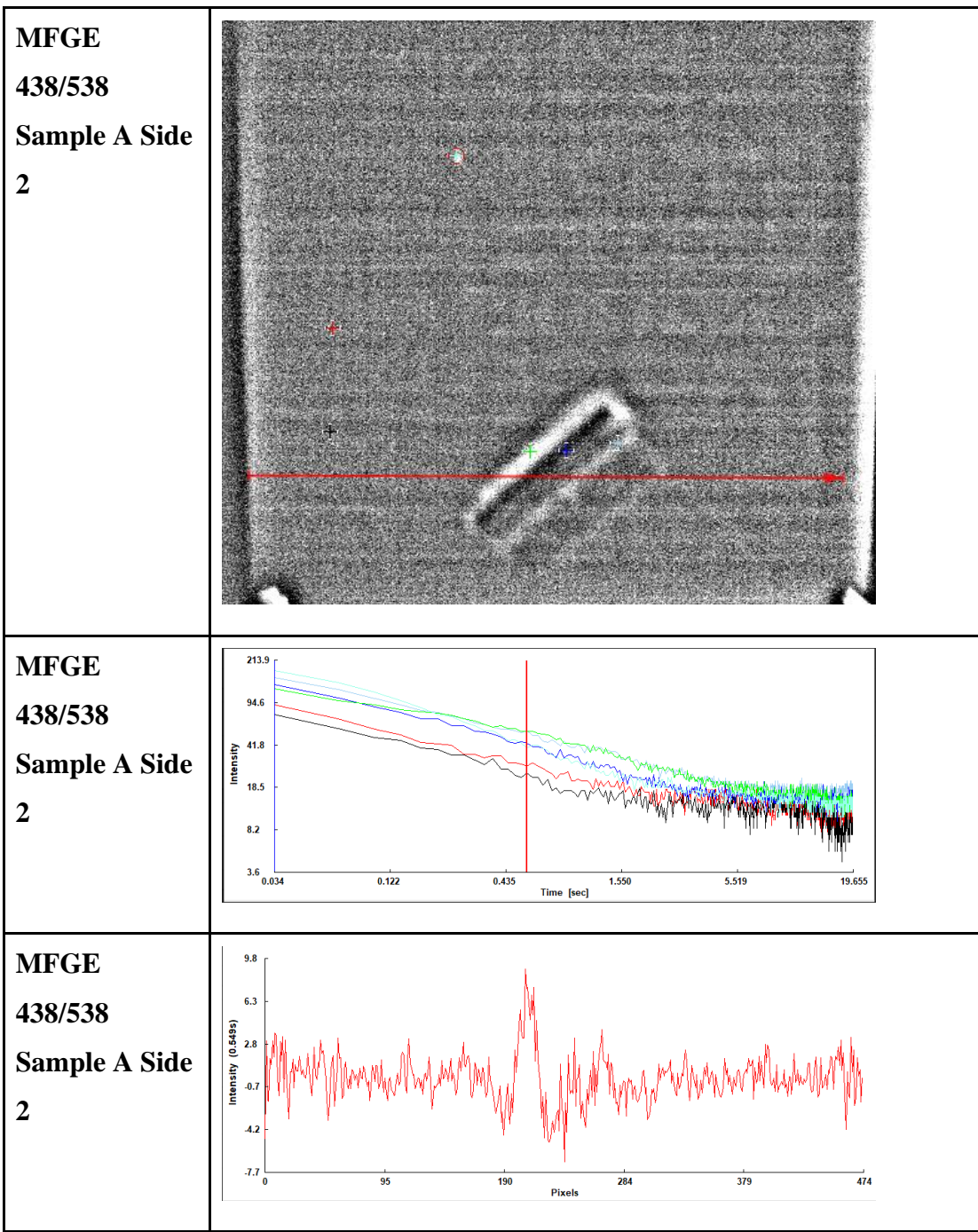
Appendix A: Non-Destructive Testing at OSU

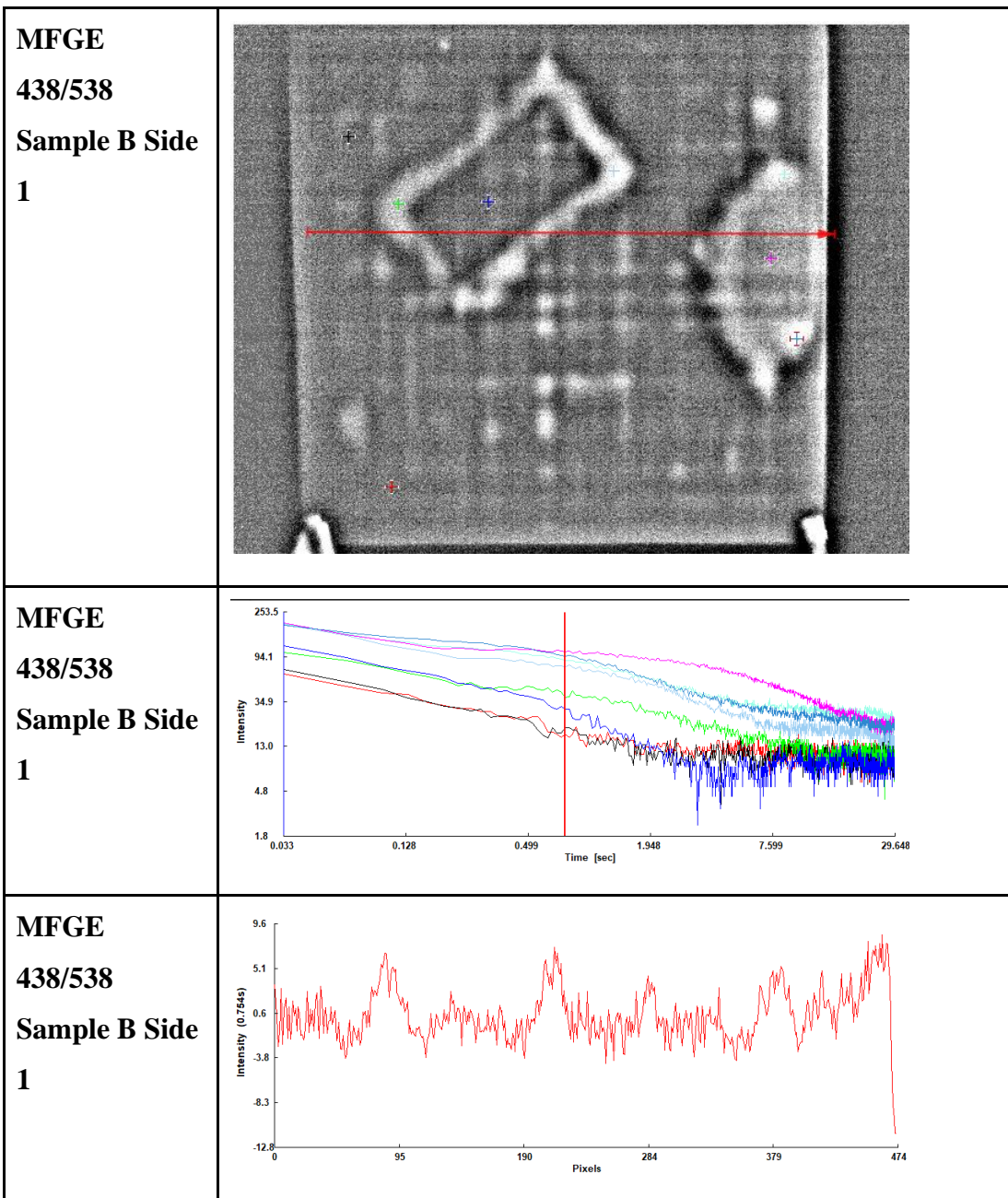
Within the OSU scope of NDT, several groups utilize the capabilities of NDT. Beginning with education, some classes, particularly MFGE 438, NDT is discussed as a means of industry testing to ensure product quality and reduce flaws in manufacturing procedures. Several projects have been set up around the use of NDT, using it to identify manufacturing procedure validity, identifying potential fail points, or observing the internal structure of various components. The TWI system is the newest addition to the repertoire of testing devices at OSU.

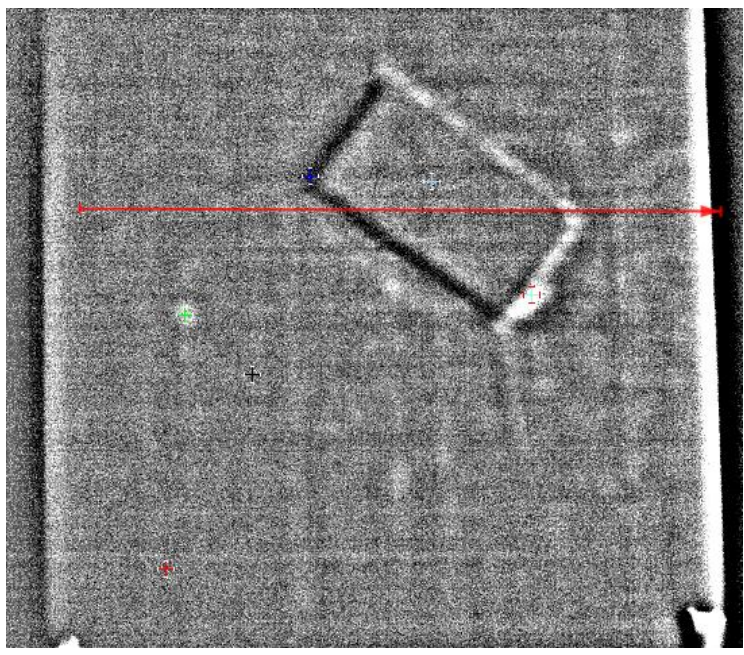
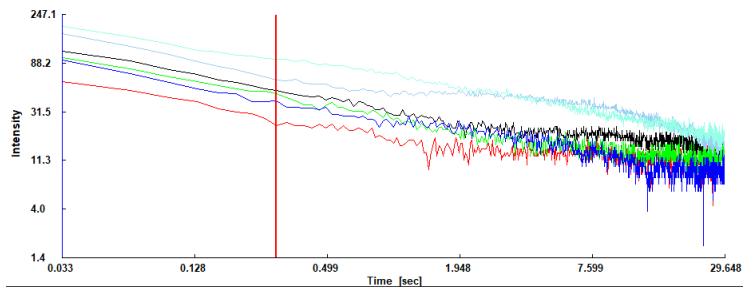
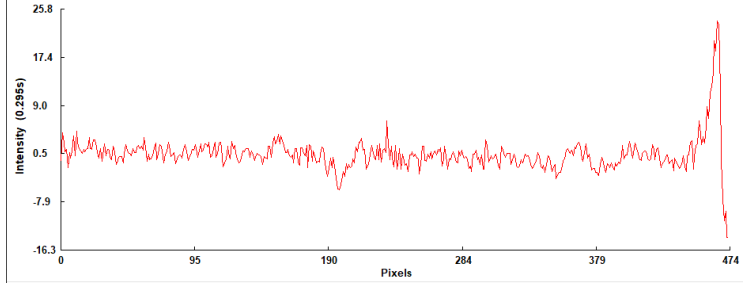
Clubs also benefit from using these systems. The racing teams at OSU utilize FRP parts often, many of which utilize some form of testing to ensure they are capable of holding up to the required loads. For example, carbon hard points are CFRP parts that are used as attachment points for various other components on the overall chassis. These hard points need to be machined from a larger laminate, which could have internal defects. Examining these laminates to identify defect location would not only allow the racing teams to cut the hardpoints from better areas, but also show if there are common areas where defects may form, indicating a problem in the manufacturing of the laminate. Aerospace clubs also use FRP components and would benefit in a similar manner.

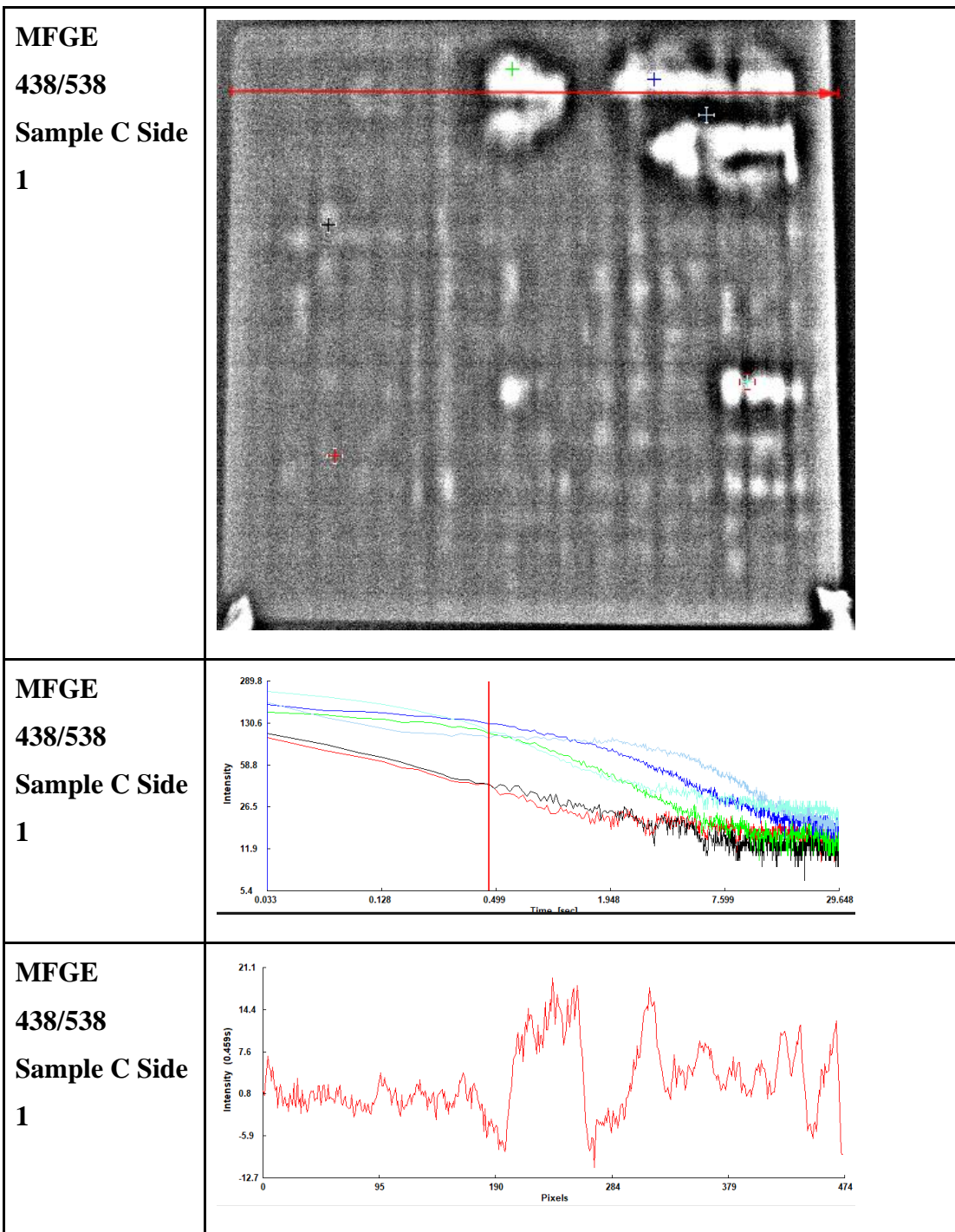
Appendix B: Other Specimens Scanned in this Study

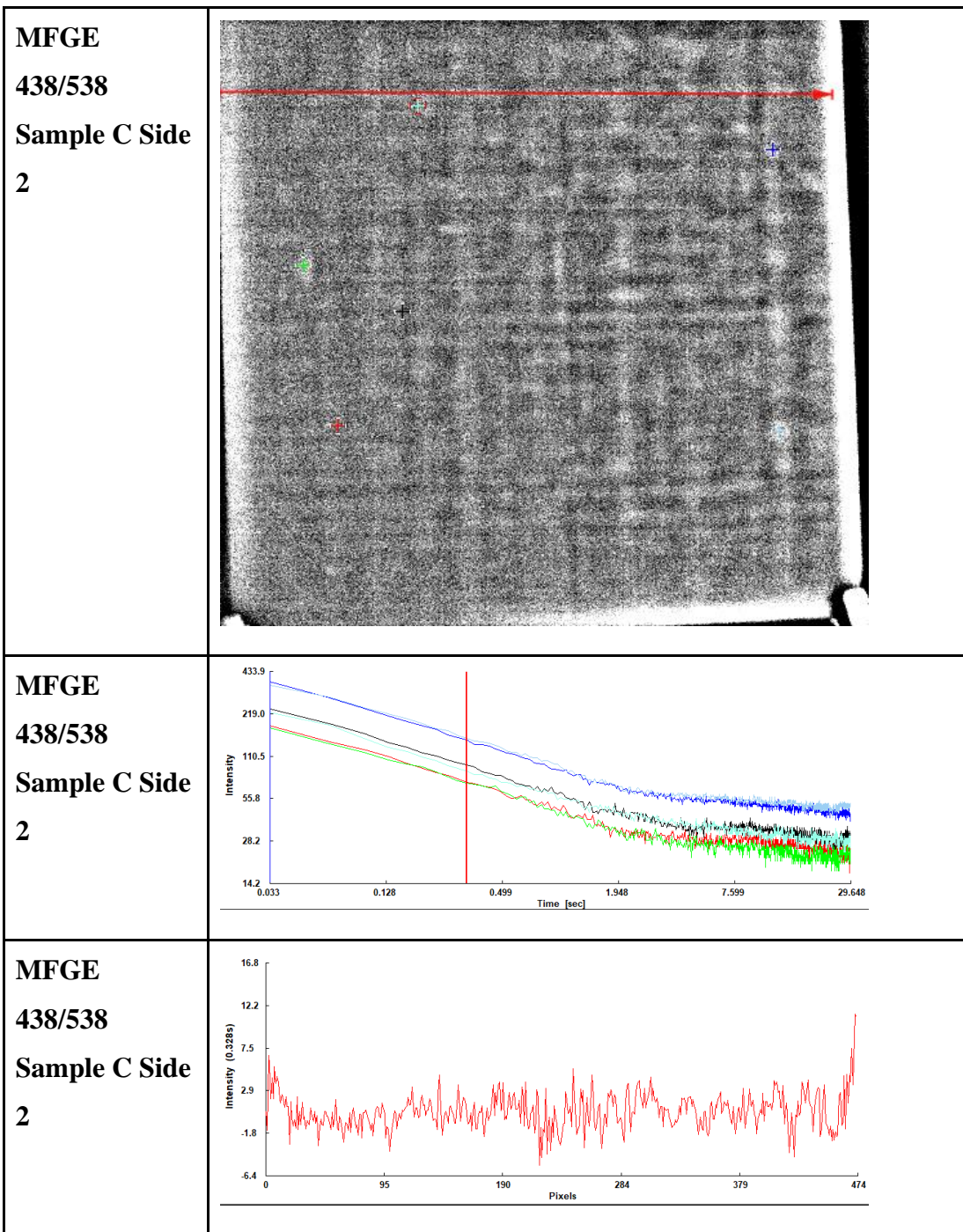


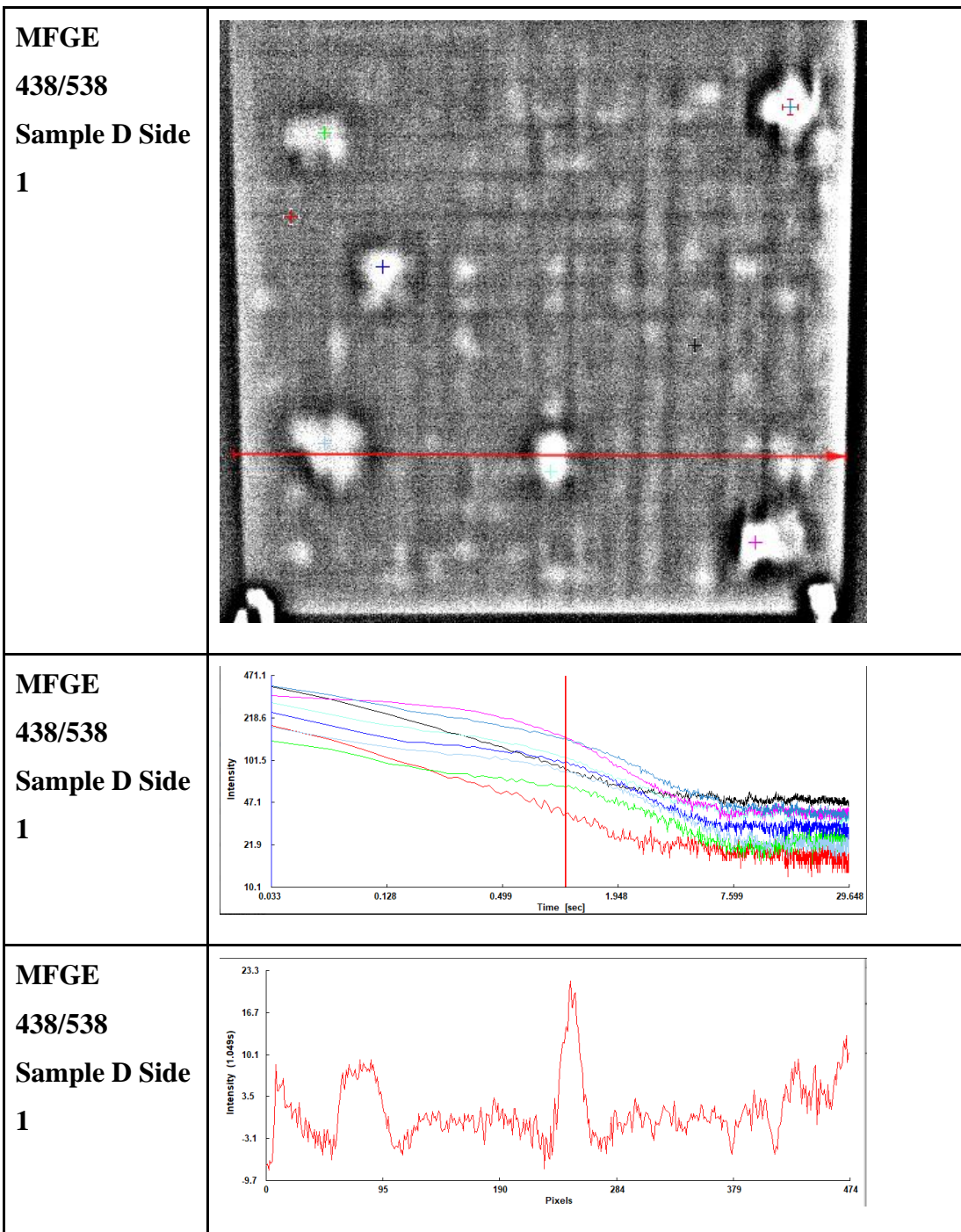


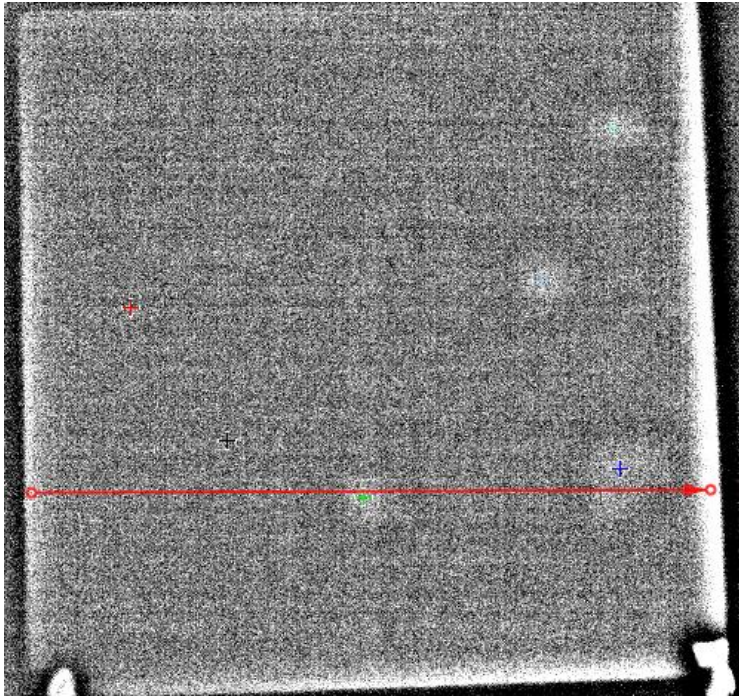
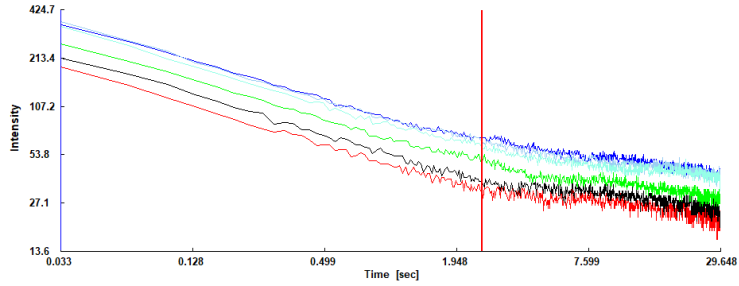
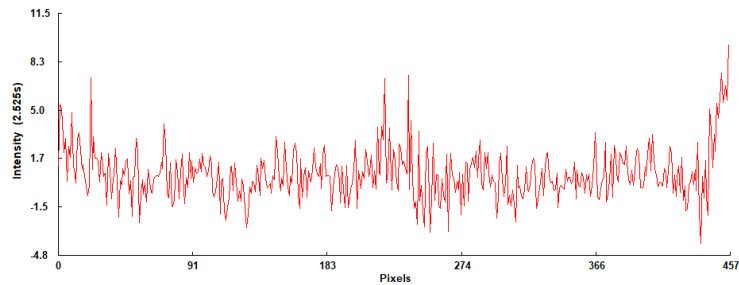


<p>MFGE 438/538 Sample B Side 2</p>	 <p>A grayscale image showing a textured surface. A red horizontal line is drawn across the middle. A blue dot is on the line, and a red square is to its right. A green crosshair is on the left, and a black crosshair is in the center.</p>
<p>MFGE 438/538 Sample B Side 2</p>	 <p>A line graph with 'Intensity' on the y-axis and 'Time [sec]' on the x-axis. The y-axis has values 1.4, 4.0, 11.3, 31.5, 88.2, and 247.1. The x-axis has values 0.033, 0.128, 0.499, 1.948, 7.599, and 29.648. Multiple colored lines (red, green, blue, black, cyan) show a general downward trend over time. A vertical red line is at 0.499 seconds.</p>
<p>MFGE 438/538 Sample B Side 2</p>	 <p>A line graph with 'Intensity (0.2985)' on the y-axis and 'Pixels' on the x-axis. The y-axis has values -16.3, -7.9, 0.5, 9.0, 17.4, and 25.8. The x-axis has values 0, 95, 190, 284, 379, and 474. A single red line shows a noisy signal that rises sharply to a peak of approximately 25.8 at the end of the pixel range.</p>







<p>MFGE 438/538 Sample D Side 2</p>	
<p>MFGE 438/538 Sample D Side 2</p>	
<p>MFGE 438/538 Sample D Side 2</p>	
<p>Table 1. <i>Other samples run in this study. These samples were manufactured for the MFGE 438/538 course. Each side was scanned, and the resulting time intensity graphs and profile graph are shown below that scan.</i></p>	

Appendix C: Tables

Material	Qualities	Results
Aluminum	<ul style="list-style-type: none"> • High conductivity • High reflectivity (if unpainted). • Easily machinable. • Readily available. 	<ul style="list-style-type: none"> • Very quick scans. • Low resolution of scan.
Fiberglass	<ul style="list-style-type: none"> • Low conductivity. • Low reflectivity. • Easily machinable. 	<ul style="list-style-type: none"> • No scans resulted in usable data.
Sandwich Panel	<ul style="list-style-type: none"> • Three layers (CFRP, Aluminum, CFRP) • Low reflectivity. • Difficult to machine. 	<ul style="list-style-type: none"> • Scans revealed the first CFRP layer struct, but did not penetrate through the entire struct.
Carbon Panels	<ul style="list-style-type: none"> • Some reflectivity. • Moderate conductivity. • Moderately machinable. 	<ul style="list-style-type: none"> • Scans showed the internal struct of panels. • Thinner panels recommended due to system limitations, but panels had best scans of all samples.

Table 2. *Qualitative summary of results.*

<u>THERMOSET</u>	<u>THERMOPLASTIC</u>
<ul style="list-style-type: none"> • Epoxy • Polyester • Phenolics • Bismaleimide (BMI) • Polyimides 	<ul style="list-style-type: none"> • Polyethylene • Polystyrene • Polypropylene • Polyetheretherketone (PEEK) • Polyetherimide (PEI) • Polyethersulfone (PES) • Polyphenylene Sulfide • Polyamide-imide (PAI)

Table 3. *The common resins used in thermoset and thermoplastic composites.*